3532 J. Med. Chem. 2010, 53, 3532–3551
DOI: 10.1021/jm901713n

Journal of Medicinal Chemistry Article

Identification of 4,5-Dihydro-1*H*-pyrazolo[4,3-*h*]quinazoline Derivatives as a New Class of Orally and Selective Polo-Like Kinase 1 Inhibitors

Italo Beria,* Dario Ballinari, Jay Aaron Bertrand, Daniela Borghi, Roberto Tiberio Bossi, Maria Gabriella Brasca, Paolo Cappella, Michele Caruso, Walter Ceccarelli, Antonella Ciavolella, Cinzia Cristiani, Valter Croci, Anna De Ponti, Gabriele Fachin, Ronald Dale Ferguson,† Jacqueline Lansen,‡ Jurgen Karl Moll, Enrico Pesenti, Helena Posteri, Rita Perego, Maurizio Rocchetti,‡ Paola Storici,§ Daniele Volpi, and Barbara Valsasina

Nerviano Medical Sciences Srl, Oncology, Viale Pasteur 10, 20014 Nerviano, (Mi), Italy. †*Present address: Merck Co. & Inc., 126 E. Lincoln Avenue, Rahway, NJ 07065.* ‡*Accelera, Nerviano Medical Sciences Srl, Viale Pasteur 10, 20014 Nerviano (MI), Italy.* §*Present address: Sincrotrone Trieste S.C.p.A., Strada Statale 14, Area Science Park, 34149 Basovizza (TS), Italy*

Received November 19, 2009

Polo-like kinase 1 (Plk1) is a fundamental regulator of mitotic progression whose overexpression is often associated with oncogenesis and therefore is recognized as an attractive therapeutic target in the treatment of proliferative diseases. Here we discuss the structure−activity relationship of the 4,5-dihydro-1*H*-pyrazolo[4,3-*h*]quinazoline class of compounds that emerged from a high throughput screening (HTS) campaign as potent inhibitors of Plk1 kinase. Furthermore, we describe the discovery of **49**, 8-{[2-methoxy-5-(4-methylpiperazin-1-yl)phenyl]amino}-1-methyl-4,5-dihydro-1*H*-pyrazolo-[4,3-*h*]quinazoline-3-carboxamide, as a highly potent and specific ATP mimetic inhibitor of Plk1 (IC_{50} = 0.007 μM) as well as its crystal structure in complex with the methylated $Plk1_{36-345}$ construct. Compound **49** was active in cell proliferation against different tumor cell lines with IC_{50} values in the submicromolar range and active in vivo in the HCT116 xenograft model where it showed 82% tumor growth inhibition after repeated oral administration.

Introduction

Mitotic cell cycle progression is tightly regulated through reversible covalent protein phosphorylation events coordinated by regulatory kinases, including members of the Polo subfamily.[1−4] Among the four Plk[a] isoforms (Plk1−4), Plk1 is the best characterized and is recognized to be a key component of the cell cycle control machinery with important roles in the mitotic entry, centrosome duplication, bipolar mitotic spindle formation, transition from metaphase to anaphase, cytokinesis, and maintenance of genomic stability.[5−9] Plk1 is often overexpressed in many different tumor types including lung, colon, prostate, ovary, breast, head and neck squamous cell carcinoma, melanoma, and overexpression often correlates with poor prognosis.[10−16] In addition, interference with Plk1 activity and/or function by a variety of methods including antisense oligonucleotides, small interfering RNA, and various dominant negatives results in tumor cell apoptosis in culture and in vivo.[17−21] Moreover, literature data report that normal cells survive Plk depletion, whereas tumor cells do not.[22] All of this evidence supports Plk1 as a valid target for anticancer drug development. Although depletion of Plk1 is sufficient to induce G2/M cell cycle block, it is not clear whether it is important or indeed beneficial to inhibit all of the other Plk isoforms. In fact, less is known concerning the physiological roles of Plk2 and Plk3 that, in contrast to Plk1, are reported to be expressed in nonproliferating differentiated post mitotic cells, like neurons, indicating a potentially better safety profile for a Plk1 specific inhibitor.[23]

Because of its essential role in cell proliferation there is a high level of interest and an increasing effort to identify and develop small-molecule inhibitors of Plks that has led to a number of different compounds which are currently under clinical investigation.[24−29]

In our effort to develop selective small-molecule Plk1 inhibitors, we identified a novel series of ATP-competitor

*To whom correspondence should be addressed. Phone: +39 0331581516. Fax: +39 03311581347. E-mail italo.beria@nervianoms.com.

[a] Abbreviations: Plk, Polo-like kinase; ABL, Abelson protein-tyrosine kinase; AKT, signal transducer and activator of transcription or protein kinase B; ALK, anaplastic lymphoma kinase; Aur, aurora; CDC, cell division cycle; CDK, cyclin dependent kinase; CK, casein kinase; CHK, Csk homologous kinase; EGFR, epidermal growth factor receptor; ERK, extracellular signal-regulated kinase; FGFR, fibroblast growth factor receptor; IGFR, insulin-like growth factor receptor; GSK, glycogen synthase kinase; IKK2, IκB kinase; IR, insulin receptor; LCK, lymphocyte-specific protein tyrosine kinase; MAP-KAPK2, mitogen activated proteinkinase-activatedprotein kinase-2; MET, high affinity tyrosine kinase receptor for hepatocyte growth factor; HGF, hepatocyte growth factor; NEK, NIMA-related kinase; NIMA, never in mitosis gene A; NIM, nim1/cdr1 protein; PAK, p-21 activated kinase; PKA, c-AMP-dependent kinase; PKC, protein kinase C; RET, receptor tyrosine kinase, STLK, serine-threonine like kinase; SULU, protein kinase 18; TRKA, catalytic receptor for the neurotrophin nerve growth factor; NGF, neurotrophin nerve growth factor; VEGFR, vascular endothelial growth factor receptor; AMP-PNP, adenylyl-imidodiphosphate tetralithium salt; NPM, nucleophosmin; TCTP, translationally controlled tumor protein; ADME, adsorption, distribution, metabolism, excretion; HLM human liver microsoms; P_{app}, apparent permeability; PAMPA, parallel artificial membrane permeation assay; EDC, *N*-(3-dimethylaminopropyl)-*N*′-ethylcarbodiimide; HOBT, 1-hydroxybenzotriazole; HOBT·NH_3, 1-hydroxybenzotriazole ammonium salt ; (±)-BINAP, (±)-2,2′-bis(diphenylphosphino)-1,1′-binaphtalene; DMF-DIPA, *N*,*N*-dimethylformamide diisopropyl acetal; DTBAD, di-*tert*-butylazodicarboxylate; $LiN(TMS)_2$, lithium bis(trimethylsilyl)amide; $Pd_2(dba)_3$, tris(dibenzylideneacetone)dipalladium(0); DMA, *N*,*N*-dimethylacetamide.

 Published on Web 04/16/2010

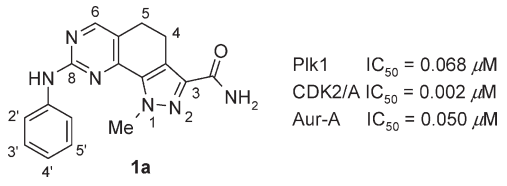

Figure 1. HTS pyrazoloquinazoline hit **1a**.

Scheme 1. Synthesis of Enaminone Intermediates **5a**−**d**[a]

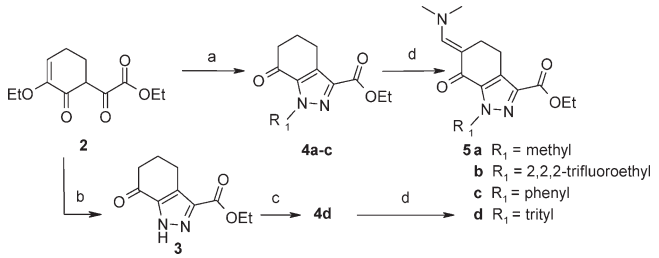

[a] Conditions: (a) hydrazine R_1NHNH_2 (**6a**−**c**), AcOH glacial, rt, 36−55%; (b) hydrazine hydrate, EtOH, reflux, 70%; (c) tritylchloride, TEA, DCM, rt, 72%; (d) DMF-DIPA, DMF, 60 °C, 54−71%.

4,5-dihydro-1*H*-pyrazolo[4,3-*h*]quinazoline derivatives and herein we report their in vitro and in vivo characterization.[30] Starting from the unselective compound **1a** (Figure 1) that was fished out from a high throughput screening (HTS) campaign, we developed compound **49**, a highly potent (Plk1 IC_{50} = 0.007 μM), selective, and orally bioavailable Plk1 inhibitor. Compound **49** showed good selectivity in a panel of more than 40 protein kinases and with more than 30-fold selectivity with respect to the Plk family members Plk2 and Plk3.

Structure−activity relationships (SAR) for this class together with data concerning the crystal structure of the selective inhibitor **49** in complex with the Plk1 kinase domain are reported below.

Chemistry

A versatile chemical strategy for the synthesis of the 4,5-dihydro-1*H*-pyrazolo[4,3-*h*]quinazoline derivatives involving the synthesis of flexible intermediates **5a**−**d** was established. Enaminones **5a**−**d** were prepared in 2/3 linear step process starting from the diketoester **2** (Scheme 1).[31] Cyclization of the diketoester **2** into the 1-substituted pyrazole derivatives **4a**−**c** was carried out in a regiospecific way by reacting suitable hydrazines **6a**−**c** in glacial acetic acid. Alternatively, reacting **2** with hydrazine hydrate followed by unselective base catalyzed alkylation of pyrazole derivative **3** with trityl chloride yielded a mixture of 1 and 2-trityl regioisomers wherein the desired intermediate **4d** was easily isolated by crystallization. Reaction of 7-oxo-tetrahydroindazole derivatives **4a**−**d** with *N*,*N*-dimethylformamide diisopropyl acetal yielded the versatile enaminones **5a**−**d**. Further elaboration of intermediates **5a**−**d** to obtain the final compounds modified at positions 1, 3, or 8 of the 4,5-dihydro-1*H*-pyrazolo[4,3-*h*]quinazoline scaffold was performed following the synthetic pathways reported in Schemes 2−4 and Figure 2. Cyclization of intermediates **5a**−**d** with phenyl guanidine carbonate at 110 °C in *N*,*N*-dimethylformamide allowed direct access to the 4,5-dihydro-1*H*-pyrazolo[4,3-*h*]quinazoline scaffold decorated at position 8 with the desired anilino moiety (**7a**−**d**) (Scheme 2). Compound **7e** was then obtained from **7d** by acidic removal of the trityl protecting group. Conversion of **7a**−**c** and **7e** into the final

Scheme 2. Synthesis of 1-Substituted 4,5-Dihydro-1*H*-pyrazolo-[4,3-*h*]quinazoline derivatives **1a**−**c**, **1e**, **1f**−**i**[a]

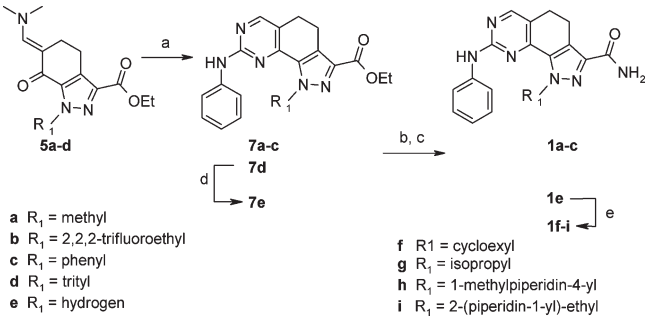

[a] Conditions: (a) phenylguanidine carbonate, DMF, 110 °C, 67−72%; (b) 1.5 M KOH/EtOH, reflux, quant; (c) EDC, HOBt·NH_3, DMF, DIPEA, rt, 56−78%; (d) TFA, DCM, rt, 80%; (e) DTBAD, Ph_3P polyimer-bound, alcohol R_1−OH (**8a**−**d**), THF, rt, 24−62%.

compounds **1a**−**c** and **1e** was obtained in two steps by hydrolysis of esters **7a**−**c** or **7e**, followed by a reaction with 1-hydroxybenzotriazole ammonium salt and EDC to introduce the primary amide function. Compound **1e** was in turn used as starting material to synthesize compounds **1f**−**i** so as to complete the series of 1-substituted pyrazole derivatives. Alkylation of **1e** with the suitable alcohols proceeded regioselectively at the position 1 of pyrazole nucleus under Mitsunobu conditions using polymer-bounded triphenyl phosphine to facilitate the workup and purification of target compounds. As previously described by Brasca and co-workers,[31] synthesis of derivatives **9**−**13** modified at the 3 position of the 4,5-dihydro-1*H*-pyrazolo[4,3-*h*]quinazoline template (Figure 2) was performed starting from ester **7a**. Modifications of the 4,5-dihydro-1*H*-pyrazolo[4,3-*h*]quinazoline scaffold at position 8 to afford compounds **19**−**49** were introduced by Buchwald−Hartwig coupling of the iodoamide **18** with suitable amines **50**−**76** or **85a**−**e** using palladium(II) acetate as catalyst and (±)-BINAP as ligand (Scheme 3). Iodoamide **18** was in turn obtained in four steps starting from enaminone **5a**, following the recently reported procedure (Figure 3).[31] Briefly, reaction of enaminone **5a** with guanidine carbonate afforded intermediate **15**, the amino group was then converted into iodo derivative **16** via diazonium salt, and finally the acid intermediate **17**, obtained from hydrolysis of ester **16**, was converted into the desired iodoamide **18**. An alternative synthesis of a limited number of derivatives (**80** and **81**) characterized by an amino or an amido residue at the position 2′ of the 8 anilino moiety was applied (Scheme 4). According to this procedure, iodoester **16** was coupled with the *N*-Boc-*o*-phenylenediamine under Buchwald−Hartwig conditions, then the protecting group was easily removed with hydrochloric acid in dioxane, generating the aminoester **78** that was coupled with acetyl chloride to yield the corresponding amido esters **79**. The final conversion of **79** into target amide **81** was achieved in a straightforward manner with 30% NH_4OH in a sealed tube at 70 °C. The same procedure was applied to the ester intermediate **78** to obtain the amide **80**. Preparation of disubstituted aniline intermediates **85a**−**e** is outlined in Schemes 5 and 6. Compounds **85a**−**b** were prepared starting from the commercially available anilines **82a**−**b**. The amino group was first protected as an acetyl derivative simply by reaction with acetic anhydride, then the 4-methylpiperazin-1-yl residue was introduced by subjecting the bromo intermediates **83a**−**b** to a Buchwald−Hartwig coupling with 4-methylpiperazine using $Pd_2(dba)_3$ as catalyst and 2-dicyclohexylphosphino-2′-(*N*,*N*-dimethylamino)-biphenyl

Scheme 3. Synthesis of 4,5-Dihydro-1*H*-pyrazolo[4,3-*h*]quinazoline Derivatives **19**−**49**[a]

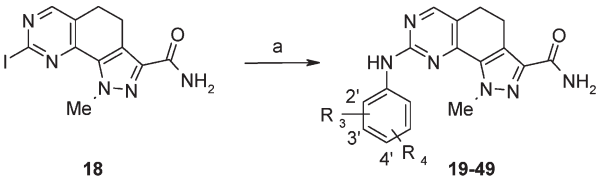

18 19-49

19 R_3 = 2'-trifluoromethyl; R_4 = H
20 R_3 = 3'-trifluoromethyl; R_4 = H
21 R_3 = 4'-trifluoromethyl; R_4 = H
22 R_3 = 2'-acetyl; R_4 = H
23 R_3 = 3'-acetyl; R_4 = H
24 R_3 = 4'-acetyl; R_4 = H
25 R_3 = 2'-methoxy; R_4 = H
26 R_3 = 3'-methoxy; R_4 = H
27 R_3 = 4'-methoxy; R_4 = H
28 R_3 = 2'-nitro; R_4 = H
29 R_3 = 3'-nitro; R_4 = H
30 R_3 = 4'-nitro; R_4 = H
31 R_3 = 2'-methyl; R_4 = H
32 R_3 = 2'-thiomethyl; R_4 = H
33 R_3 = 2'-methylamino; R_4 = H
34 R_3 = 2'-fluoro; R_4 = H
35 R_3 = 2'-isopropyl; R_4 = H
36 R_3 = 2'-methoxycarbonyl; R_4 = H
37 R_3 = 2'-carbamoyl; R_4 = H
38 R_3 = 2'-sulfamoyl; R_4 = H
39 R_3 = 2'-phenyl; R_4 = H
40 R_3 = 2'-phenoxyl; R_4 = H
41 R_3 = 2'-benzyl; R_4 = H
42 R_3 = 2'-phenylamino; R_4 = H
43 R_3 = 2'-benzoyl; R_4 = H
44 R_3 = 2'-phenylsulphanyl; R_4 = H
45 R_3 = 2'-acetyl; R_4 = 3'-(4-methylpiperazin-1-yl)
46 R_3 = 2'-acetyl; R_4 = 4'-(4-methylpiperazin-1-yl)
47 R_3 = 2'-acetyl; R_4 = 5'-(4-methylpiperazin-1-yl)
48 R_3 = 2'-methoxy; R_4 = 4'-(4-methylpiperazin-1-yl)
49 R_3 = 2'-methoxy, R_4 = 5'-(4-methylpiperazin-1-yl)

[a] Conditions: (a) $Pd(OAc)_2$, (±)-BINAP, K_2CO_3, amines (**50**−**76**; **85a**−**e**), DMF, 80 °C, 7−77%.

Scheme 4. Synthesis of 2′ Anilino Derivatives **79** and **81**[a]

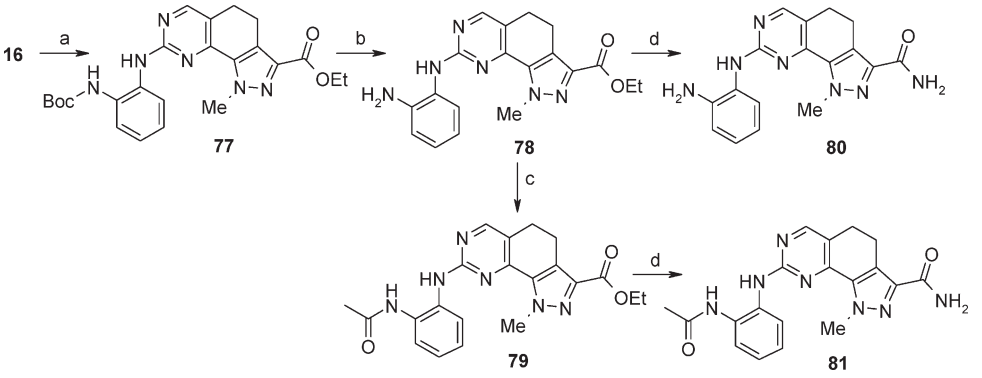

[a] Conditions: (a) $Pd(OAc)_2$, (±)-BINAP, K_2CO_3, *N*-Boc-*o*-phenylenediamine, 61%; (b) 4N HCl/dioxane, DCM, rt, 96%; (c) acetyl chloride, DIPEA, rt, 72%; (d) 30% NH_4OH, EtOH, sealed tube, 70 °C, 17−64%.

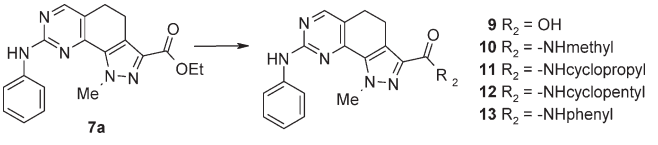

Figure 2. Compounds modified at the position **3**.

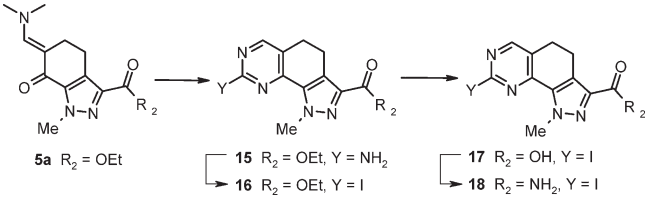

Figure 3. Synthesis of intermediate **18**.

as ligand. Final removal of the amino protecting group under acid conditions afforded intermediates **85a**−**b** (Scheme 5). An alternative approach was applied for the synthesis of **85c**−**d**. The first step (Scheme 5) foresaw the installation of the 4-methylpiperazin-1-yl residue by reacting 4-methylpiperazine under either palladium catalyzed Buchwald−Hartwig coupling conditions, in the case of the less reactive 4-bromo-1-methoxy-2-nitro-benzene **83c**, or by high temperature nucleophilic substitution conditions for the more reactive 1-(2-chloro-6-nitro-phenyl)-ethanone **83d**. Final reduction of both nitro derivatives **84c**−**d** was carried out under catalytic palladium conditions, with hydrogen in a Parr apparatus under 35 psi presssure generating **85c** and under atmospheric pressure with cyclohexene as hydrogen source producing **85d**. Amine intermediate **85e** was prepared subjecting the commercially available 1-(4-fluoro-2-hydroxy-phenyl)-ethanone **86** to nucleophilic substitution with 4-methyl-piperazine at high temperature (Scheme 6). Then, phenol derivative **87** was converted into the target aniline **85e** by a one-pot reaction with 2-bromo-2-methylpropionamide and NaOH in *N,N*-dimethylacetamide via a Smiles rearrangement.[32]

Results and Discussion

In the HTS campaign for the discovery of small-molecule inhibitors of Plk1, compound **1a**[31] belonging to the 4,5-dihydro-1*H*-pyrazolo[4,3-*h*]quinazoline class emerged as an interesting hit. Despite strong cross activity with others kinases,

Scheme 5. Synthesis of Amino Intermediates **85a−d**[a]

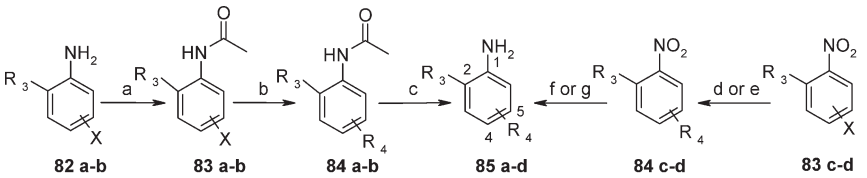

[a] Conditions: (a) acetic anhydride, rt, 42−51%; (b) $Pd_2(dba)_3$, 1 M $LiN(TMS)_2$/THF, 4-methylpiperazine, 2-dicyclohexylphosphino-2′-(*N*,*N*-dimethylamino)-biphenyl, reflux, 53−91%; (c) HCl conc, EtOH, reflux, 45%-quant; (d) 4-methylpiperazine, $Pd(OAc)_2$, K_3PO_4, 2-dicyclohexylphosphino-2′-(*N*,*N*-dimethylamino)-biphenyl, THF, reflux, 55%; (e) 4-methylpiperazine, 120 °C sealed tube, 68%; (f) cyclohexene, 10% Pd/C, HCl conc, THF/H_2O/EtOH, 70 °C, 95%; (g) 10% Pd/C, H_2, 35 psi, MeOH, 90%.

Scheme 6. Synthesis of Amino Intermediate **85e**[a]

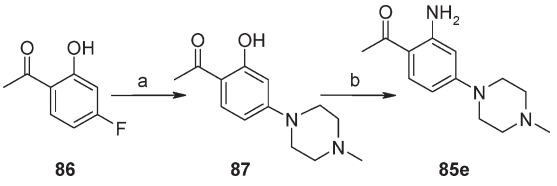

[a] Conditions: (a) 4-methylpiperazine, 130 °C, quant; (b) NaOH, DMA, 2-bromo-2-methylpropanamide, rt. then NaOH, 100 °C, 30%.

e.g., Aur-A and CDK2/A, inhibitor **1a** was selected for a chemistry expansion aimed at defining the structure activity relationship for this novel class and at improving both the selectivity profile and the pharmacokinetic properties. In particular, the effect of modifications at positions 1, 3, and 8 of the 4,5-dihydro-1*H*-pyrazolo[4,3-*h*]quinazoline scaffold will be discussed in more depth.

Compounds modified at position 1 of the 4,5-dihydro-1*H*-pyrazolo[4,3-*h*]quinazoline template together with biochemical activity against Plk1, CDK2/A, Aur-A kinases and in vitro cell proliferation cytotoxicity on A2780 cell lines are reported in Table 1. According to this data, substitutions at position 1 of pyrazole ring did not improve the selectivity vs CDK2/A or Aur-A kinases. In contrast, the introduction of bulky groups in this position had dramatic effects on the Plk1 activity. Specifically, the compounds wherein the methyl substituent was removed (**1e**) or replaced with the cyclohexyl moiety (**1f**) showed a maintained or increased cytotoxicity (IC_{50} = 0.10 and 0.55 μM, respectively), but a decreased Plk1 activity (Plk1 IC_{50} = 0.248 and 0.143 μM, respectively) with respect to progenitor **1a** (Plk1 IC_{50} = 0.068 μM). Replacement of methyl with a small flexible trifluoroethyl residue (**1b**) resulted in increased Plk1 activity (IC_{50} = 0.006 μM) but decreased cellular activity (IC_{50} = 2.75 μM) with respect to **1a**. A decrease from 6- to more than 100-fold in Plk1 biochemical activity was observed with the increase of the substituent's complexity (**1c**, **1 g−i**). On the basis of these data, the methyl group was identified as the best residue at the position 1 of the 4,5-dihydro-1*H*-pyrazolo[4,3-*h*]quinazoline core in terms of biochemical and cellular activity.

Exploration of the 3 position was performed with the synthesis of a set of compounds wherein the primary amide residue of hit **1a** was replaced with ethyl ester function (**7a**), carboxylic acid residue (**9**), or with secondary amides (**10−13**). Activity results reported in Table 2 show that most of these

Table 1. SAR: Variation of R_1 Substitution[a]

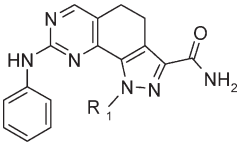

Compd	R_1	IC_{50}, μM			
		Plk1	CDK2/A	Aur-A	A2780
1a	Me	0.068	0.002	0.050	0.50
1b		0.006	0.005	0.042	2.75
1c		>10	0.015	2.360	>10
1e	H	0.248	0.002	0.092	0.10
1f		0.143	0.007	0.169	0.55
1g	*i*-Pr	0.430	0.046	1.392	0.31
1h	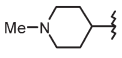	>10	0.104	>10	4.71
1i	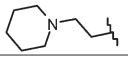	>10	0.030	2.848	0.89

[a] IC_{50} values are the average of $n \geq 2$.

modifications significantly decreased Plk1 activity. Even the simple methyl amide derivative **10** showed a 60-fold loss of activity in the Plk1 biochemical assay and 5-fold reduction in cell proliferation potency with respect to the parent compound **1a**. The only derivative that maintained the progenitor's activity was the carboxylic acid **9**, however, its selectivity profile vs CDK2/A and Aur-A was not improved. Moreover, cellular activity of **9** was decreased 5-fold with respect to **1a**, probably due to the reduced capability of the carboxylic acid to cross the cellular membrane with respect to the primary amide as confirmed by the low value in the Caco-2 permeability assay of **9** with respect to **1a** (P_{app} **1a** = 58.3 × 10^{-6}cm/s; P_{app} **9** = 2.7 × 10^{-6} cm/s).

Exploration at position 8 of the scaffold was initiated by evaluating the influence of substituents at positions 2′, 3′, or 4′ of the anilino residue. Analysis of the biochemical data reported in Table 3 shows that in an homogeneous series,

Table 2. SAR: Variation of R_2 Substituent[a]

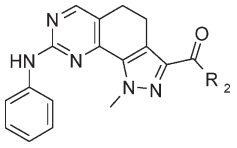

compd	R_2	IC_{50}, μM			
		Plk1	CDK2/A	Aur-A	A2780
1a	NH_2	0.068	0.002	0.050	0.50
7a	OEt	> 10	0.251	> 10	2.79
9	OH	0.110	0.003	0.016	2.54
10	NHMe	4.215	0.019	0.312	2.63
11	NHcyclopropyl	> 10	0.081	0.213	3.82
12	NHcyclopentyl	> 10	3.900	> 10	> 10
13	NHPh	> 10	0.574	> 10	> 10

[a] IC_{50} values are the average of $n \geq 2$.

Table 3. SAR: Variation of R_3 Substitution[a]

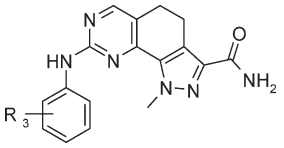

compd	R_3	Plk1 (IC_{50}, μM)	CDK2/A (IC_{50}, μM)	CDK2/A/Plk1 ratio	Aur-A (IC_{50}, μM)	Aur-A/Plk1 ratio	A2780 (IC_{50}, μM)
1a	H	0.068	0.002	0.030	0.050	0.740	0.50
19	*o*-CF_3	0.432	0.306	0.708	> 10	> 23	> 10
20	*m*-CF_3	0.051	0.006	0.118	> 10	> 196	1.49
21	*p*-CF_3	0.872	0.003	0.003	0.270	0.310	0.25
22	*o*-Ac	0.346	1.263	3.656	> 10	> 28	> 10
23	*m*-Ac	0.100	0.002	0.020	0.176	1.767	0.09
24	*p*-Ac	0.197	0.002	0.009	0.116	0.589	0.04
25	*o*-OMe	0.042	0.041	0.969	0.607	14.452	0.94
26	*m*-OMe	0.135	0.005	0.035	0.158	1.164	1.05
27	*p*-OMe	0.256	0.004	0.016	0.128	0.499	0.05
28	*o*-NO_2	0.488	0.209	0.428	> 10	> 20	3.49
29	*m*-NO_2	> 10	0.005	< 0.001	> 10		1.68
30	*p*-NO_2	> 10	0.014	< 0.001	> 10		1.96

[a] IC_{50} values are the average of $n \geq 2$.

substitution at positions 3′ and 4′ of the phenyl ring was inefficient to increase Plk1 selectivity, especially against CDK2/A, as revealed by the substantially unmodified CDK2A/Plk1 ratio or Aur-A/Plk1 ratio for the compound pairs **20**−**21**, **23**−**24**, or **26**−**27** in comparison with **1a**. A unique behavior was shown by the nitro derivatives **29** and **30**, wherein despite a retention of activity on CDK2/A, a dramatic loss of activity was observed for Plk1 and Aur-A. As far as the 2′ substituted derivatives are concerned, the Plk1 activity was either maintained (**25**) or slightly decreased (**19**, **22**, **28**). However, more importantly, a general increase of selectivity against both CDK2/A and Aur-A was evident. In particular, the 2′-methoxy derivative **25** showed a marginal gain in terms of selectivity vs both CDK2/A (CDK2/A/Plk1 ratio from 0.03 to 0.97) and vs Aur-A (Aur-A/Plk1 ratio from 0.74 to 14.45) and a maintained cytotoxic activity on A2780 with respect to **1a**. An even more positive trend was shown by the 2′-acetyl derivative **22**, with an increased selectivity with respect to **1a** against both CDK2/A (CDK2/A/Plk1 ratio from 0.03 to 3.65) and Aur-A (Aur-A/Plk1 ratio from 0.74 to > 28) but with loss of cytotoxicity on A2780. The high cytotoxicity shown by the unselective compounds **21**, **23**, **24**, and **27** (IC_{50} = 0.25, 0.09, 0.04, and 0.05 μM, respectively) in comparison with **1a** (IC_{50} = 0.5 μM) suggested that cellular activity of these compounds could be due to the inhibition by other kinases as, e.g., CDK2/A and Aur-A. The maintained cytotoxicity and the improved Plk1 selectivity shown by compound **25** in comparison with the unselective hit **1a** indicates that the ortho position is key for obtaining active and selective Plk1 inhibitors. In light of these positive results, a deeper investigation was performed to map the chemical space at position 2′ of the anilino moiety with the synthesis of a set of compounds differing in both electronic characteristics and steric bulk (Table 4). The data confirmed **25** as the most promising compound in terms of cellular activity on A2780 cell line, potency against Plk1 (IC_{50} = 0.042 μM), and improved, but still low, selectivity vs Aur-A and CDK2/A with respect to progenitor **1a**. Compound **25**, however, did not show selectivity vs Plk2 and Plk3 isoforms. The lack of selectivity against Plk2 and Plk3 was shared by all compounds reported in Table 4, indicating that this position is probably not suitable in achieving selectivity for Plk1 isoform; furthermore, all compounds, with the exception of **80**, demonstrated solubility at pH 7 below 30 μM. It is worth noting that

Table 4. SAR: Variation of R_3 Substitution[a]

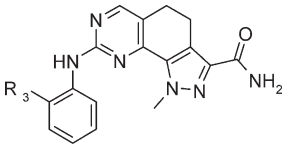

		IC$_{50}$, μM						
compd	R_3	Plk1	Plk2	Plk3	CDK2/A	Aur-A	A2780	solubility at pH 7, μM
1a	H	0.068	0.009	0.014	0.002	0.050	0.50	3
19	CF_3	0.432	0.109	0.095	0.306	> 10	> 10	4
22	Ac	0.346	0.261	0.103	1.263	> 10	> 10	2
25	OMe	0.042	0.024	0.013	0.041	0.607	0.94	3
31	Me	0.015	0.002	0.006	0.003	0.605	0.80	3
32	SMe	0.097	0.014	0.016	0.142	> 10	6.86	2
33	NHMe	0.110	0.012	0.011	0.017	2.900	7.54	23
34	F	0.125	0.027	0.037	0.007	1.181	0.67	3
35	*i*-Pr	0.365	0.509	0.146	0.358	> 10	> 10	2
36	CO_2Me	1.117	nd	nd	1.448	> 10	> 10	2
37	$CONH_2$	2.076	nd	nd	2.746	> 10	> 10	< 1
38	SO_2NH_2	3.733	nd	nd	1.120	> 10	8.30	4
39	Ph	1.565	nd	nd	1.347	> 10	> 10	< 1
40	OPh	0.278	2.666	0.051	1.900	> 10	> 10	< 1
41	benzyl	0.943	nd	nd	0.571	> 10	> 10	< 1
42	NHPh	0.949	nd	nd	0.442	> 10	5.85	< 1
43	benzoyl	1.969	nd	nd	> 10	> 10	> 10	< 1
44	SPh	2.033	nd	nd	> 10	> 10	> 10	< 1
80	NH_2	0.150	0.012	0.013	0.007	2.497	2.92	190
81	NHAc	2.523	2.104	0.049	1.037	> 10	3.93	16

[a] IC$_{50}$ values are the average of $n \geq 2$. nd, not determined.

Table 5. SAR: Variation of R_3 and R_4 Substitution[a]

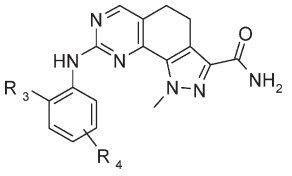

			IC$_{50}$, μM						
compd	R_3	R_4	Plk1	Plk2	Plk3	CDK2/A	Aur-A	A2780	solubility at pH 7, μM
1a	H	H	0.068	0.009	0.014	0.002	0.050	0.50	3
45	Ac	3′-(4-methyl-piperazin-1-yl)	2.051	> 10	> 10	1.121	> 10	> 10	170
46	Ac	4′-(4-methyl-piperazin-1-yl)	0.464	> 10	2.292	> 10	> 10	> 10	83
47	Ac	5′methyl-piperazin-1-yl)	0.109	> 10	> 10	> 10	> 10	0.762	18
48	OMe	4′-(4-methyl-piperazin-1-yl)	0.040	0.082	0.066	0.082	> 10	0.146	> 225
49	OMe	5′-(4-methyl-piperazin-1-yl)	0.007	0.238	0.450	0.355	> 10	0.009	170

[a] IC$_{50}$ values are the average of $n \geq 2$.

introduction of medium/large moieties (**36**−**44** and **81**) in the 2′ position, with the exception of phenoxy derivative **40**, was detrimental not only for Plk1 inhibition (IC$_{50} \geq 0.9\,\mu$M) but also for the others kinases (IC$_{50} > 0.4\,\mu$M) (Table 4). On the contrary, small groups were well tolerated by Plk1 (**19**, **22**, **25**, **31**−**35**, and **80**) as confirmed by the only 6-fold loss of activity on the enzyme for **19** (IC$_{50} = 0.432\,\mu$M) and the 4-fold increased activity shown by **31** (IC$_{50} = 0.015\,\mu$M) when compared with **1a** (IC$_{50} = 0.068\,\mu$M). A significant modification in terms of potency and selectivity was achieved by the introduction of an additional substituent on the anilino moiety at position 8 (Table 5). Complete loss of biochemical activity for all the kinases and loss of cellular proliferation activity were obtained when the 4-methylpiperazino residue was introduced at the position 3′ of the 8-anilino substituent (**45**). However, encouraging results were obtained by introducing the 4-methylpiperazino substituent at the position 4′ of the anilino moiety (**46** and **48**). These derivatives not only maintained acceptable Plk1 activity but they also maintained or even improved the selectivity toward CDK2/A and Aur-A. In addition, improved selectivity against Plk2 and Plk3 was also achieved (compare **46** and **48** with **22** and **25**, respectively). Particularly interesting were the data for **47** and **49**, wherein the 4-methylpiperazino moiety was placed at the 5′ position of the 8-anilino appendix. Derivative **49** proved to be the best compound of the series, showing antiproliferative activity in the low nanomolar range in the A2780 cell line (IC$_{50} = 0.009\,\mu$M), good activity on Plk1 (IC$_{50} = 0.007\,\mu$M),

Table 6. Kinase Selective Profile of Compound **49**

kinase	IC_{50}, (μM)[a]	kinase	IC_{50}, (μM)[a]
Plk1	0.007 ± 0.003	CDK2/A	0.355 ± 0.167
CK2	0.115 ± 0.045	Plk3	0.450 ± 0.101
CDK1/B	0.160 ± 0.029	VEGFR3	0.587 ± 0.230
CDK5/p25	0.219 ± 0.092	PDGFR	0.954 ± 0.317
Plk2	0.238 ± 0.043	KIT	1.904 ± 0.860
CDK2/E	0.347 ± 0.127	others[b]	> 10 (31 kinases)

[a] Data are reported as a mean ± standard deviation (n = 2). [b] c-ABL, AKT1, ALK, Aur-A, Aur-B, CDC7, CDK7, CDK4/D1, CHK1, EGFR1, ERK2, FGFR1, IGFR1, GSK3β, IKK2, IR, LCK, MAP-KAPK2, MET, NEK-6, NIM, PAK4, PDK1, PKAα, PKCβ, P38α, RET, STLK2, SULU1, TRKA, and VEGFR2.

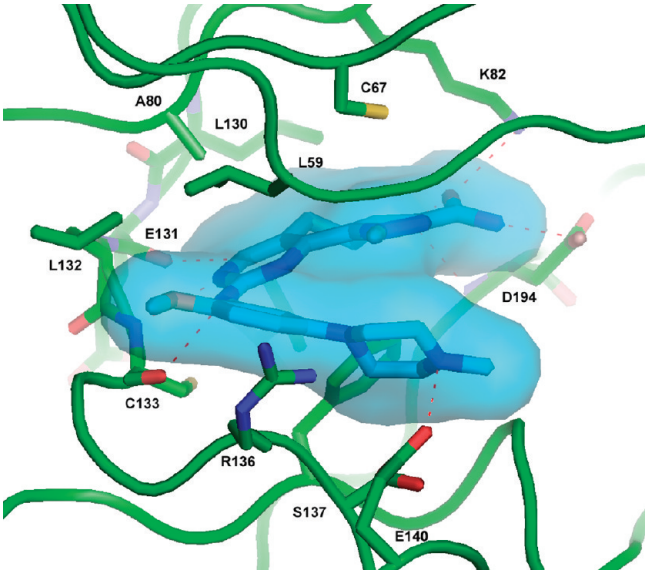

Figure 4. Compound **49** bound to Plk1. Hydrogen bonds are shown as red dashed lines.

and a high level of selectivity against Plk2, Plk3, CDK2/A, and Aur-A (0.238, 0.450, 0.355, and > 10 μM, respectively). Furthermore, the introduction of 4-methylpiperazino residue also proved to be beneficial to the compound's solubility that, in the case of **49**, resulted more than 50-fold with respect to **1a**. The high level of selectivity of compound **49** was also confirmed using a larger panel of more than 40 kinases, giving selectivity ratios that ranged from 16-fold to > 1400-fold (Table 6).

A multiple construct approach was applied in order to obtain the crystal structure of the Plk1 kinase domain in complex with proprietary inhibitors. Specifically, out of 32 constructs that were cloned and tested for expression, 12 were purified on a large scale and subjected to extensive crystallization trials. However, initial efforts to obtain crystals of these constructs, both in the presence and absence of inhibitors, were unsuccessful. As a salvage approach, selected constructs were methylated and subjected to subsequent rounds of crystallization screening. In the end, this approach proved to be successful and crystals were obtained of methylated $Plk1_{36-345}$ bound to the nonhydrolyzable ATP analogue AMP-PNP. Interestingly, the crystal form that we obtained independently is the same as the one subsequently reported in the literature even though the crystallization conditions were different.[33] Remarkably, a zinc ion was observed in a crystal contact while no zinc was intentionally added to the solution providing these first crystals. A similar result concerning the unexpected presence of zinc in the crystals was also reported by Kothe and co-workers.[33] Moreover, among several structures subsequently solved, a methylated lysine could be unambiguously identified in only one structure (Lys257, data not shown). By soaking crystals of the methylated-$Plk1_{36-345}$:AMP-PNP complex with compound **49**, we were able to replace the AMP-PNP with the inhibitor, as indicated by its well-defined electron density in the structure.[34] As expected, **49** binds in the cleft between the N- and C-terminal lobes with

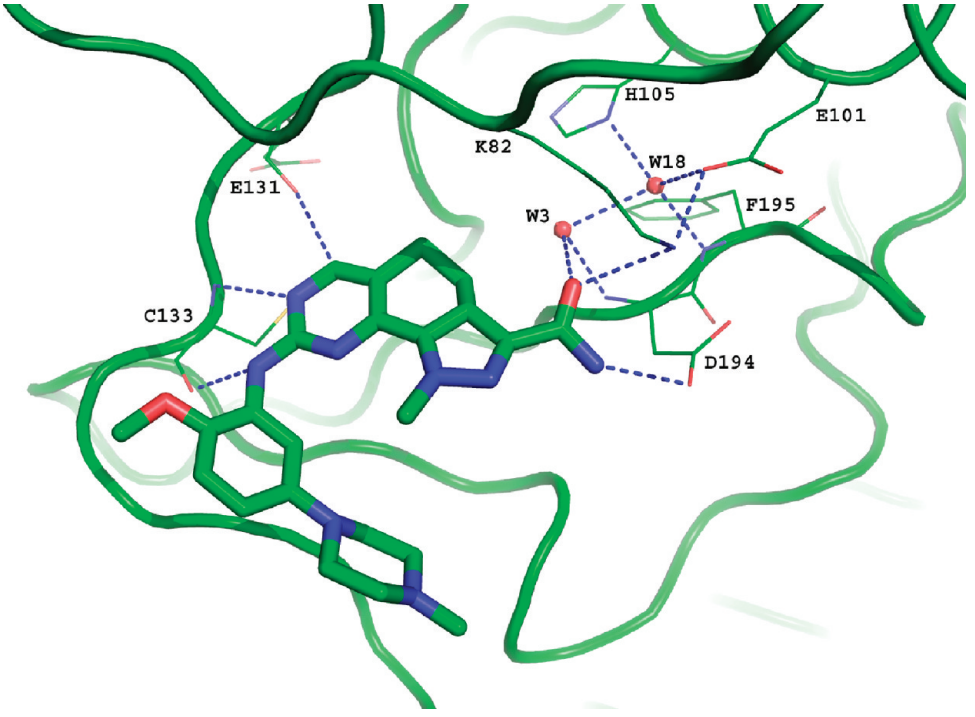

Figure 5. Hydrogen bonding network that links compound **49** to the regulatory spine residues His105 and Phe195.

the aminoquinazoline core, making three hydrogen bonds with the main chain atoms of Glu131 and Cys133 in the hinge region (Figure 4). The glycine-rich loop folds down tightly over the inhibitor, with Leu59 sitting above the aromatic group in position 8 and Cys67 above the pyrazolo ring. More specifically, the aromatic group in position 8 is sandwiched between Leu59 (above) and Arg136 (below) and the substituents extend along the lower part of the hinge in opposite directions. The inhibitor's amide moiety points toward the DFG motif of the enzyme (residues 194−196) and is part of an extensive network of hydrogen bonds (Figure 5). The amide is directly bound to the side chains of Asp194 and Lys82 as well as to the main chain nitrogen of Asp194 through a bridging water molecule (W3). Interestingly, a conserved structural water molecule (W18)[35] bridges together W3, the conserved Glu101 of αC helix and Phe195 and His105, two residues belonging to the regulatory spine of protein kinases.[36] Not suprisingly, the structural results, as elaborated below, are consistent with our key SAR findings that include the importance of the amide and the substituents on the aromatic group in position 8. Specifically, the amide hydrogen bonding network and the shape of this region of the binding site can explain the decreased activity for compounds carrying an ester function (**7a**) or secondary amido residues (**10**−**13**) at position 3 of the template with respect to the primary amide derivative (**1a**). The 2′-methoxy group of **49** is accommodated in a small pocket close to the hinge residue Leu132, and this moiety is believed to play a critical role in obtaining selectivity against kinases bearing a residue bulkier than leucine in this position, such as those present in Aurora-A and CDK2/A. It is worth noting that a similar observation have been made for the methoxy group of the inhibitor BI-2536.[37] A contribution to selectivity and to potency comes from the methylpiperazine moiety at position 5′ of the aniline residue (compare **22** with **47** and **25** with **49**). This substituent fits very well in a pocket lined mainly by residues of the kinase C-lobe, including Ser137 that forms the "floor" of this pocket (Figure 6). The corresponding amino acids in Aurora-A and CDK2/A are the larger Thr217 and Asp86, respectively. On the basis of the crystal structures of Aurora-A and CDK2/A with compounds of the same chemical class as **49** (proprietary data not shown), a clash would be likely to occur between these residues and the methylpiperazine substituent, explaining at least partially the observed selectivity against these two enzymes. Moreover, Glu140 of Plk1 is well positioned to establish a polar interaction with one of the piperazine nitrogens (Figure 6). This, together with the optimal fitting of the methylpiperazine into its binding pocket, could explain the gain in potency given by this substituent. Interestingly, the amino acid corresponding to Glu140 of Plk1 is a histidine in both Plk2 and Plk3. Because the chemical properties of histidine are likely to hamper an interaction with a positively charged nitrogen, this feature might be the basis of the selectivity displayed by compounds **47** and **49** for Plk1 with respect to Plk2 and Plk3. A similar idea concerning the role of Plk1 residue Glu140 in the selectivity versus Plk2 and Plk3 has been recently proposed

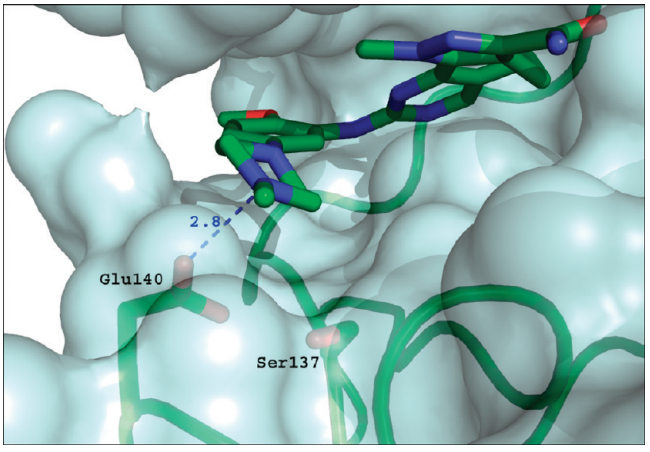

Figure 6. Binding pocket of the methylpiperazino substituent of **49**, shown as a Connolly surface. The indicated distance for the interaction between Glu140 and **49** is in Ångstroms.

Table 7. Antiproliferative Activity of Compound **49**

cell line	origin	IC_{50}, (μM)[a]	cell line	origin	IC_{50}, (μM)[a]
A2780	ovary	0.009	A431	epithelial	0.010
A2780/cis	ovary resistant to cis platinum	0.011	MCF7	mammary	0.044
A2780/ADR	ovary resistant to adriamycin	0.057	NCI-H929	myeloma	0.004
A2780 1A9	ovary	0.014	OPM-2	myeloma	0.004
A2780 1A9/PTX22	ovary resistant to patlitaxel	0.016	NHDF	human fibroblast	0.073
PANC-1	pancreatic	0.022	KARPAS-299	lymphoma	0.005
MIA-PaCa-2	pancreatic	0.044	Jurkat	lymphoma	0.008
HCT-116	colon	0.025	KU812	leukemia	0.003
LoVo	colon	0.066	HEL	erythroleukemia	0.005
LoVo/Dx	colon resistant to doxorubicin	0.078			

[a] IC_{50} values are reported as the mean of 2−3 experiments with a coefficient of variation below 35%.

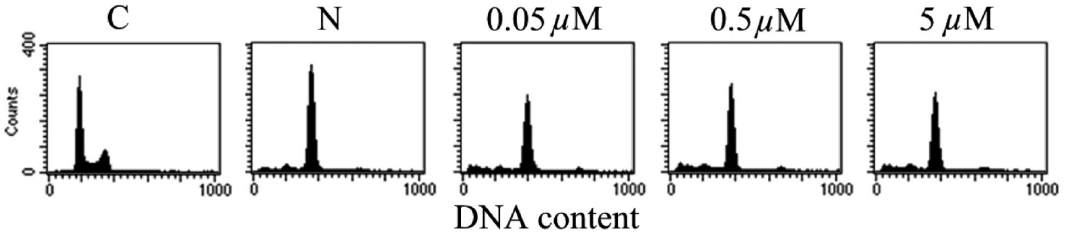

Figure 7. Flow cytometry analysis of **49** in A2780 cells. Cells were treated for 24 h with different doses of **49** (0.05 μM, 0.5 μM and 5 μM). DNA profile of untreated (C) and Nocodazole (N) treated cells are also reported.

based on a homology model of Plk1 bound to a thiophene inhibitor.[38]

On the basis of its favorable biochemical profile together with high potency in A2780 cell lines (IC_{50} = 9 nM) and good solubility (170 μM at pH 7), compound **49** was selected for further in vitro and in vivo testing. In vitro antiproliferative activity of **49** was evaluated in a broad panel of cell lines (Table 7). Compound **49** proved to be a potent inhibitor of cell growth in vitro across a wide range of solid as well as hematological tumor cell lines. Compound **49** was also active in resistant cell lines like A2780 human ovarian adenocarcinoma cell line, which is resistant to *cis*-platinum (A2780/cis IC_{50} = 0.011 μM), A2780 human ovary adenocarcinoma cell line ,which is resistant to adriamycin (A2780/ADR IC_{50} = 0.057 μM), or the A2780 human ovary adenocarcinoma resistant to paclitaxel (A2780 1A9/PTX22 IC_{50} = 0.016 μM), displaying comparable activity to that found in the parental cell line (A2780 IC_{50} = 0.009 μM and A2780 1A9 IC_{50} = 0.014 μM, respectively). The same behavior was observed in the LoVo human colon adenocarcinoma cell line resistant to doxorubicin (LoVo/Dx IC_{50} = 0.078 μM) compared to the parental line (LoVo IC_{50} = 0.066 μM). The mechanism of action of compound **49** was checked by flow cytometry analysis evaluating the percentage of cells with a 4N DNA content in A2780 cells. After 24 h treatment a clear G2/M block was observed by fluorescence activated cell sorting (FACS) (Figure 7). Analysis of cell cycle markers on A2780 cells at different dosages of **49** was also evaluated by Western blot. An increase in pSer10 histone H3 and pThr199 NPM in agreement with a mitotic block mechanism was observed in a dose-dependent manner (Figure 8). The specific Plk1 mechanism of action of **49** was reinforced by the clear down-regulation of phosphorylation of Ser46 in TCTP, a reported substrate of Plk1.[39] Apoptosis induction was evaluated in two different cell lines, A2780 and HCT116 cells, which were treated at two different doses of **49** (0.5 μM and 1.5 μM) for 24 h followed by growth of cells for additional 24 h in the absence of compound. A G2/M cell cycle block was shown by flow cytometry after 24 h compound treatment, while after

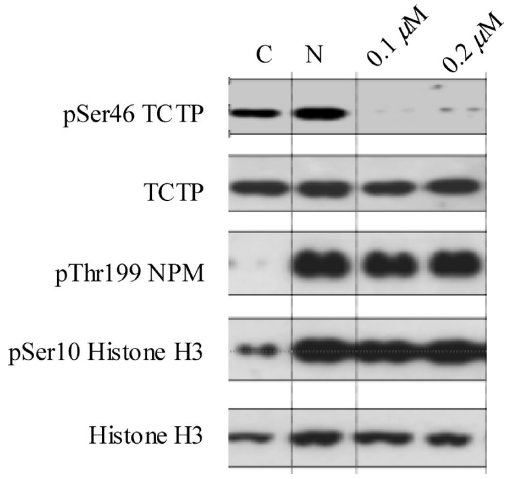

Figure 8. Western blot analysis of **49** on A2780 cells. Cells were treated with **49** at two different doses (0.1 and 0.2 μM) for 24 h. Shown are untreated (C) and Nocodazole (N) treated cells. The Plk specific marker (pSer46 TCTP) as well as mitotic markers (pSer10 Histone H3 and pThr199 NPM) were evaluated. Total TCTP was used as loading control.

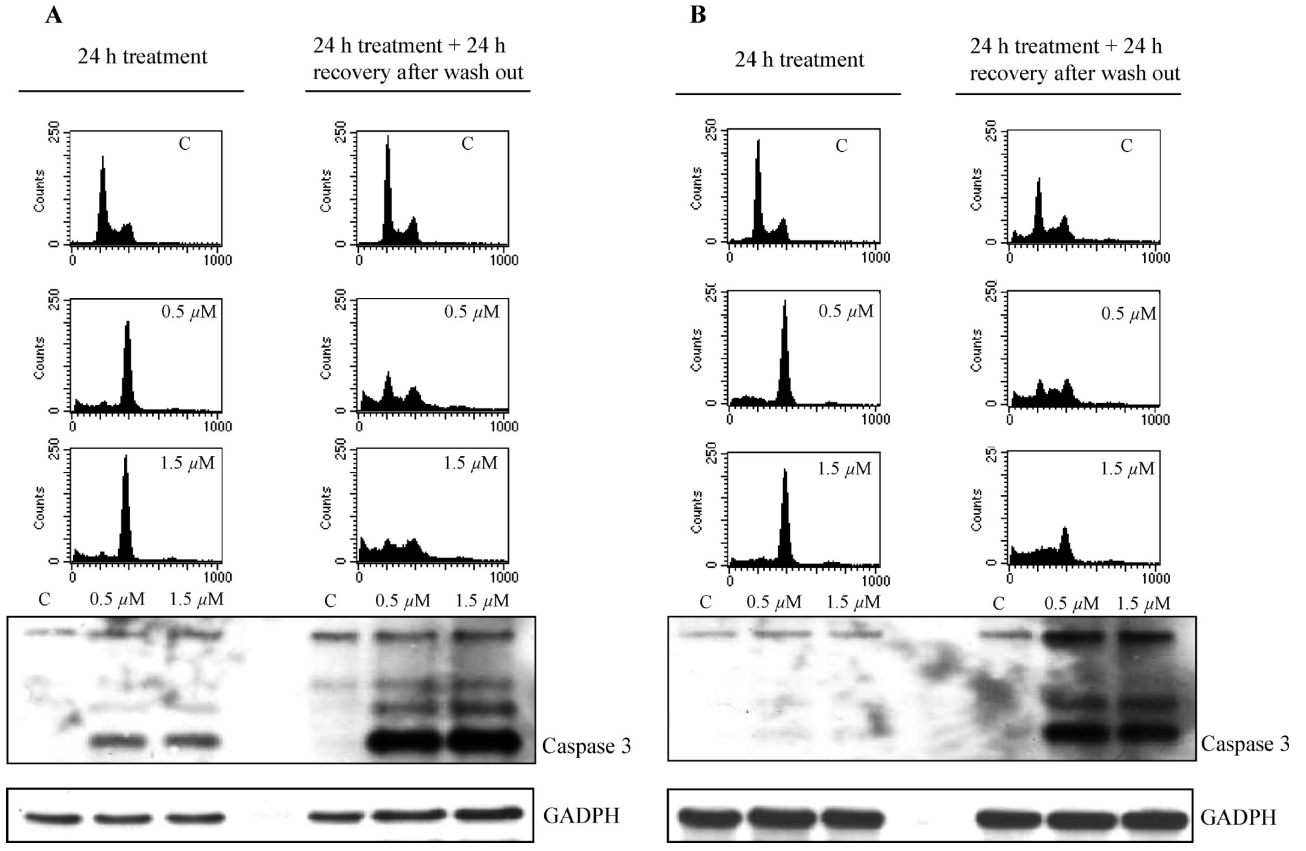

Figure 9. Flow cytometry and Western blot analysis of A2780 (A) or HCT116 (B) cells treated for 24 h with 0.5 μM or 1.5 μM of **49** and after additional 24 h in the absence of compound. Expression of GAPDH was used as loading control.

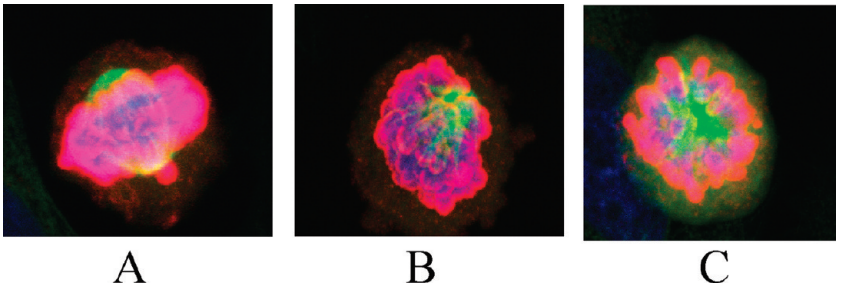

Figure 10. Aberrant monopolar spindles upon inhibition of Plk1. Immunofluorescence pictures of representative U2OS cells during mitosis. Control (A), siRNA targeting Plk1 (NM005030, sense strand 5′-CGAGCUGCUUAAUGACGAG) as assessed 72 h after transfection (B), and treatment with 0.3 μM of compound **49** for 72 h (C). Blue, DNA; red, pSer10 histone H3; green, α-tubulin. Images were taken with an objective 40× by using a confocal laser mounted on a Zeiss microscopy (Radiance 2000, Biorad).

Table 8. In Vitro ADME Parameters of Compound **49**

	permeability		metabolic stability	
solubility 10% Tween 80 (mg/mL)	Caco-2 (P_{app} 10^{-6} cm/s)	PAMPA[a] (P_{app} 10^{-6} cm/s)	Cl_{int} (L/h/kg) rat hepatocyte (1 μM)	Cl_{int} (L/h/kg) HLM[b] (1 μM)
2.7	29.4	50.0	12.5	0.6

[a] Parallel artificial membrane permeability. [b] Human liver microsomes.

Table 9. Mean ± Standard Deviation Pharmacokinetic Parameters of Compound **49** Following iv Bolus Single Dose and Oral Single Dose in Harlan nu/nu Mice[a]

in vivo ADME parameters									
PK data (iv), dose[b]: 10 mg/kg					PK data (po), dose[b]: 10 mg/kg				
C_{max} (μM)	AUC_∞ (μM·h)	CL (L/h/kg)	Vss (L/kg)	$t_{1/2}$ (h)	C_{max} (μM)	t_{max} (h)	AUC_∞ (μM·h)	$t_{1/2}$ (h)	F[c] (%)
6.07 ± 1.27	6.51 ± 0.60	3.55 ± 0.43	2.43 ± 0.31	0.73 ± 0.04	0.85 ± 0.16	0.42 ± 0.14	1.36 ± 0.17	0.86 ± 0.17	13.7

[a] n = 3 animals per study. [b] Dosed as HCl in situ salt/glucosate. [c] Bioavailability.

an additional 24 h of recovery in the absence of compound, a clear caspase-3 induction was observed. Also a high percentage of cells within the subG1 population, which is indicative of massive apoptosis, was observed at all tested doses. These data suggest that the compound acts by an initial prolonged mitotic block, followed by an induction of apoptosis through activation of caspases (Figure 9A,B).

To access the phenotype of cells treated with **49**, U2OS cells were treated either with **49** or transfected with siRNA specific for Plk1 and assessed for markers for the mitotic spindle (α-tubulin), DNA, and pSer10 histone H3, using confocal microscopy. Clearly, the presence of aberrant, predominantly monopolar spindles was observed in both siRNA transfected cells and in **49** treated cells, which is in line with the expected mechanism of action of inhibitng Plk-1, while normal bipolar spindles were present in control cells (Figure 10).

In addition, in vitro physicochemical ADME properties were evaluated showing that compound **49** had an excellent metabolic stability, both in rat (Cl_{int} = 12.5 L/h/kg at 1 μM) and in human liver hepatocytes (Cl_{int} = 0.6 L/h/kg) (Table 8). Inhibitor **49** also displayed high permeability in PAMPA as well as in Caco-2 cell models (P_{app} 10^{-6} cm/s = 50 and 29.4, respectively), suggesting a possible oral bioavailability for the compound. In vivo pharmacokinetic properties were assessed in rodent species following intravenous (iv) and oral (po) dosing (Table 9). In mice, after iv dosing, **49** showed medium/high clearance (3.55 L/h/kg) and a volume of distribution about three times the mouse total body water (2.43 L/kg), indicating a good tissue distribution. Plasma levels were detectable up to 6 h post dosing, with a half-life of 0.7 h and an AUC of 6.51 μM·h. After po dosing, the t_{max} of compound **49** was found to be reached at 0.4 h, with a terminal half-life

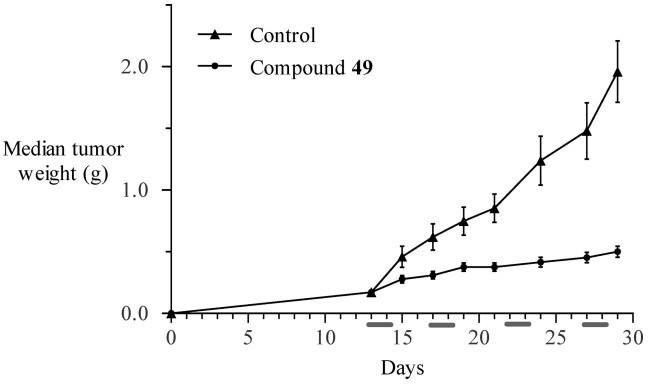

Figure 11. Compound **49** shows antitumor activity (TGI = 82%) in rodent BALB/c nu/nu mice carrying subcutaneous HCT116 human colon adenocarcinoma. Mice were treated with either vehicle or **49** by oral administration (schedule 90 mg/kg 1, 2 daily × 4 cycles). Data are represented as mean ± SEM.

compatible to that found after iv administration and with a modest but acceptable oral bioavailability (F = 13.7%).

In vivo efficacy of compound **49** was evaluated in male BALB/c nu/nu mice subcutaneously xenografted with HCT116 colon adenocarcinoma cells. The compound was administered by oral route at 90 mg/kg, day 1−2 on a weekly schedule × 4 cycles showing good antitumor activity (TGI_{max} 81%) and good tolerability (Figure 11).

Conclusion

In summary, we have reported the discovery of a new 4,5-dihydro-1*H*-pyrazolo[4,3-*h*]quinazoline class of ATP competitive Plk1 inhibitors. Optimization of the HTS hit

compound **1a** led to 8-{[2-methoxy-5-(4-methylpiperazin-1-yl)phenyl]amino}-1-methyl-4,5-dihydro-1*H*-pyrazolo[4,3-*h*]-quinazoline-3-carboxamide inhibitor **49**. The crystal structure of methylated $Plk1_{36-345}$ construct in complex with several inhibitors together with the SAR information acquired in the optimization of the class have been fruitful to identify key structural components necessary to achieve Plk1 activity and kinase selectivity. This resulted in compound **49**, which is active on Plk1 in the low nM range, selective vs Plk2, Plk3, and a panel of 39 unrelated Plk kinases, with high in vitro potency across a wide range of solid as well as hematological tumor cell lines. The compound has shown modest but acceptable oral bioavailability resulting in a plasma exposure sufficient to achieve good tumor growth inhibition in subcutaneous HCT-116 tumor xenograft and it was well tolerated after repeated oral administration.

Experimental Section

1. Chemistry. All solvents and reagents, unless otherwise stated, were high grade, commercially available, and used without further purification. All experiments dealing with moisture-sensitive compounds were conducted under dry nitrogen or argon. Organic solutions were evaporated using a Heidolph WB 2001 rotary evaporator at 15−20 mmHg. Thin-layer chromatography was performed on Merck silica gel 60 F_{254} precoated plates. Column chromatography was conducted either under medium pressure on silica (Merck silica gel 40−63 μm) or on prepacked silica gel cartridges (Biotage). Components were visualized by UV light (λ: 254 nm) and by iodine vapor. NMR spectra were recorded in DMSO-d_6 or $CDCl_3$ on a Varian Inova 400 spectrometer operating at 400.50 MHz for ^{1}H and on a Varian Inova 500 spectrometer operating at 499.75 MHz for ^{1}H and at 125.67 MHz for ^{13}C. Residual solvent signal was used as reference (δ = 2.50 or 7.27 ppm for ^{1}H and δ = 39.5 ppm for ^{13}C). Chemical shifts (δ) are reported in parts per million (ppm) and coupling constants (J) in Hz. The following abbreviations are used for multiplicities: s = singlet, bs = broad signal, d = doublet, t = triplet, m = multiplet, dd = doublet of doublets. Standard two-dimensional sequences provided by Varian (gradient-enhanced HSQC and HMBC) were used to assign carbons.

Electrospray (ESI) mass spectra were obtained on a Finnigan LCQ ion trap. Unless otherwise specified, all final compounds were homogeneous (purity of not less than 95%), as determined by high-performance liquid chromatography (HPLC). HPLC-UV-MS analyses, used to assess compound purity, were carried out combining the ion trap MS instrument with HPLC system SSP4000 (Thermo Separation Products) equipped with an autosampler LC Pal (CTC Analytics) and UV6000LP diode array detector (UV detection 215−400 nm). Instrument control, data acquisition and processing were performed with the Xcalibur 1.2 software (Finnigan). HPLC chromatography was run at room temperature, and 1 mL/min flow rate, using a Waters X Terra RP 18 column (4.6 mm × 50 mm; 3.5 μm). Mobile phase A was ammonium acetate 5 mM buffer (pH 5.5 with acetic acid): acetonitrile 90:10, and mobile phase B was ammonium acetate 5 mM buffer (pH 5.5 with acetic acid):acetonitrile 10:90; the gradient was from 0 to 100% B in 7 min then hold 100% B for 2 min before requilibration. ESI(+) high resolution mass spectra (HRMS) were obtained on a Waters Q-Tof Ultima directly connected with micro HPLC 1100 Agilent as previously described.[40]

Synthesis of compounds **1a**, **2**, **4a**, **5a**, **7a**, **9**−**13**, **15**−**18** was previously described,[31] compounds **4a**−**c**, **8a**−**d**, **14a**−**d**, and **50**−**76** are commercially available.

Ethyl 7-Oxo-4,5,6,7-tetrahydro-1*H*-indazole-3-carboxylate (3). To a solution of ethyl (3-ethoxy-2-oxocyclohex-3-en-1-yl)-(oxo)acetate **2** (10.0 g, 41.62 mmol) in ethanol (100 mL), hydrazine hydrate (2.1 mL, 67.4 mmol) was added and the solution stirred at reflux for one day. The solvent was evaporated and the residue redissolved with DCM (20 mL). The organic layer was washed with water (20 mL), dried over anhydrous sodium sulfate, and evaporated to dryness. The crude residue was triturated with diethyl ether and filtered to give the title compound (6.0 g, 70%). ^{1}H NMR (DMSO-d_6) δ ppm 1.30 (t, J = 7.1 Hz, 3H), 2.03−2.09 (m, 2H), 2.52 (t, J = 6.1 Hz, 2H), 2.91 (t, J = 6.1 Hz, 2H), 4.29 (q, J = 7.1 Hz, 2H), 14.41 (bs, 1H). LCMS (ESI) m/z 209 $(M + H)^+$.

Ethyl 7-Oxo-1-(2,2,2-trifluoroethyl)-4,5,6,7-tetrahydro-1*H*-indazole-3-carboxylate (4b). To a solution of **2** (10.0 g, 41,62 mmol) in glacial acetic acid (15 mL), trifluoroethylhydrazine (70% in water, 6.3 mL, 50.0 mmol) was added. The mixture was stirred at room temperature for 6 h. The solvent was evaporated and the crude redissolved in water (20 mL), made basic with 30% NH_4OH, and extracted with DCM (2 × 50 mL). The combined organic layers were then dried over anhydrous sodium sulfate and evaporated to dryness. The crude residue was triturated with diethyl ether and filtered to give the title compound (6.64 g, 55%). ^{1}H NMR (DMSO-d_6) δ ppm 1.31 (t, J = 7.1 Hz, 3H), 2.05−2.09 (m, 2H), 2.59 (dd, J = 6.1, 7.3 Hz, 2H), 2.95 (t, J = 6.1 Hz, 2H), 4.31 (q, J = 7.1 Hz, 2H), 5.48 (q, J = 8.8 Hz, 2H). LCMS (ESI) m/z 291 $(M + H)^+$. HRMS (ESI) calcd for $C_{12}H_{13}F_3N_2O_3 + H^+$ 291.0951, found 291.0941.

Ethyl 7-Oxo-1-phenyl-4,5,6,7-tetrahydro-1*H*-indazole-3-carboxylate (4c). By employment of the above-described procedure, starting from **2** and using the suitable substituted hydrazine, the compound **4c** was prepared. Yield, 36%. ^{1}H NMR (DMSO-d_6) δ ppm 1.32 (t, J = 7.1 Hz, 3H), 2.08−2.15 (m, 2H), 2.56 (dd, J = 5.7, 7.5 Hz, 2H), 3.03 (t, J = 6.1 Hz, 2H), 4.34 (q, J = 7.1 Hz, 2H), 7.51 (s, 5H). LCMS (ESI) m/z 285 $(M + H)^+$; HRMS (ESI) calcd for $C_{16}H_{16}N_2O_3 + H^+$ 285.1234, found 285.1236.

Ethyl 7-Oxo-1-trityl-4,5,6,7-tetrahydro-1*H*-indazole-3-carboxylate (4d). To a solution of **3** (2.1 g, 10.00 mmol) in DCM (100 mL), triethylamine (1.59 mL, 11.00 mmol) and triphenylmethyl chloride (3.2 g, 11.00 mmol) were added. The solution was stirred at room temperature for 6 h, then DCM (50 mL) was added and finally washed with water (30 mL). The combined organic layers were dried over anhydrous sodium sulfate and evaporated to dryness. The crude residue was triturated with diethyl ether and filtered to give the title compound (3.2 g, 72%). ^{1}H NMR (DMSO-d_6) δ ppm 1.25 (t, J = 7.0 Hz, 3H), 1.90−1.97 (m, 2H), 2.18 (dd, J = 5.5, 7.5 Hz, 2H), 3.00 (t, J = 6.1 Hz, 2H), 4.26 (q, J = 7.0 Hz, 2H), 6.90−7.35 (m, 15H). LCMS (ESI) m/z 468 $(M + NH_4)^+$. HRMS (ESI) calcd for $C_{29}H_{26}N_2O_3 + NH_4^+$ 468.2282, found 468.2289.

Ethyl 6-[(Dimethylamino)methylidene]-7-oxo-1-(2,2,2-trifluoroethyl)-4,5,6,7-tetrahydro-1*H*-indazole-3-carboxylate (5b). To a solution of **4b** (10.0 g, 34.45 mmol) in DMF (100 mL) *N*,*N*-dimethylformamide diisopropyl acetal (12.4 mL, 86.17 mmol) was added. The reaction mixture was stirred at 60 °C for 8 h. The solvent was then evaporated in vacuo and the product crystallized from EtOH to give the title compound (16.9 g, 71%). ^{1}H NMR (DMSO-d_6) δ ppm 1.30 (t, J = 7.1 Hz, 3H), 2.85 (t, J = 6.3 Hz, 2H), 2.93 (t, J = 6.3 Hz, 2H), 3.14 (s, 6H), 4.30 (q, J = 7.1 Hz, 2H), 5.60 (q, J = 9.0 Hz, 2H), 7.55 (s, 1H). LCMS (ESI) m/z 346 $(M + H)^+$.

Compounds 5c and 5d. By employment of the above-described procedure, starting from **4c** and **4d**, the compounds **5c** and **5d** were prepared.

Ethyl 6-[(Dimethylamino)methylidene]-7-oxo-1-phenyl-4,5,6,7-tetrahydro-1*H*-indazole-3-carboxylate (5c). Yield, 60%. ^{1}H NMR (DMSO-d_6) δ ppm 1.32 (t, J = 7.1 Hz, 3H), 2.83 (t, J = 6.3 Hz, 2H), 2.95 (t, J = 6.3 Hz, 2H), 3.12 (s, 6H), 4.30 (q, J = 7.1 Hz, 2H), 7.40 (s, 1H), 7.51 (s, 5H). LCMS (ESI) m/z 340 $(M + H)^+$.

Ethyl 6-[(Dimethylamino)methylidene]-7-oxo-1-trityl-4,5,6,7-tetrahydro-1*H*-indazole-3-carboxylate (5d). Yield, 54%. ^{1}H NMR (DMSO-d_6) δ ppm 1.26 (t, J = 7.1 Hz, 3 H), 2.74−2.79 (m, 2 H), 2.85−2.90 (m, 2 H), 3.10 (s, 6H), 4.24 (q, J = 7.1 Hz, 2 H), 6.90−7.30 (m, 15 H), 7.43 (s, 1 H). LCMS (ESI) m/z 506

$(M + H)^+$. HRMS (ESI) calcd for $C_{32}H_{31}N_3O_3 + H^+$ 506.2444, found 506.2439.

Ethyl 8-(Phenylamino)-1-(2,2,2-trifluoroethyl)-4,5-dihydro-1*H*-pyrazolo[4,3-*h*]quinazoline-3-carboxylate (7b). Phenyl guanidine carbonate (2.13 g, 13.31 mmol) was added to a suspension of **5b** (3.58 g, 10.81 mmol) in DMF (30 mL) and stirred at 110 °C for 6 h. After the mixture was cooled, the solvent was evaporated and the residue was dissolved in DCM and washed with water. The organic layer was then dried over sodium sulfate and concentrated. The residue was triturated with diethyl ether and filtered to give **7b** as a white solid (4.51 g, 67%). ^{1}H NMR (DMSO-d_6) δ ppm 1.35 (t, J = 7.1 Hz, 3H), 2.89 (t, J = 7.1 Hz, 2H), 3.04 (t, J = 7.1 Hz, 2H), 4.38 (q, J = 7.1 Hz, 2H), 5.55 (q, J = 8.8 Hz, 2H), 6.89−6.94 (m 1H), 7.24−7.29 (m, 2H), 7.79−7.83 (m, 2H). LCMS (ESI) m/z 418 $(M + H)^+$. HRMS (ESI) calcd for $C_{20}H_{18}F_3N_5O_2 + H^+$ 418.1486, found 418.1472.

Compounds 7c and 7d. By employment of the above-described procedure, starting from **5c** and **5d**, the compounds **7c** and **7d** were prepared.

Ethyl 1-Phenyl-8-(phenylamino)-4,5-dihydro-1*H*-pyrazolo-[4,3-*h*]quinazoline-3-carboxylate (7c). Yield, 62%. ^{1}H NMR (DMSO-d_6) δ ppm 1.34 (t, J = 7.1 Hz, 3H), 2.93 (t, J = 7.3 Hz, 2H), 3.04 (t, J = 7.3 Hz, 2H), 4.35 (q, J = 7.1 Hz, 2H), 6.75 (t, J = 7.19 Hz, 1H), 6.72−6.77 (m, 1H), 6.87−6.92 (m, 2H), 6.98−7.02 (m, 2H), 7.54−7.62 (m, 5H), 8.47 (s, 1H), 9.36 (s, 1H). LCMS (ESI) m/z 412 $(M + H)^+$. HRMS (ESI) calcd for $C_{24}H_{21}N_5O_2 + H^+$ 412.1768, found 412.1763.

Ethyl 8-(Phenylamino)-1-trityl-4,5-dihydro-1*H*-pyrazolo[4,3-*h*]-quinazoline-3-carboxylate (7d). Yield, 22%. ^{1}H NMR (DMSO-d_6) δ ppm 1.28 (t, J = 7.1 Hz, 3H), 2.69 (t, J = 6.7 Hz, 2H), 3.01 (t, J = 6.7 Hz, 2H), 4.26 (q, J = 7.1 Hz, 2H), 6.83 (m, 1H), 6.96−7.06 (m, 8H), 7.14 (m, 2H), 7.19−7.28 (m, 9H), 7.41 (bs, 1H), 8.18 (s, 1H). LCMS (ESI) m/z 578 $(M + H)^+$. HRMS (ESI) calcd for $C_{37}H_{31}N_5O_2 + H^+$ 578.2551, found 578.2545.

Ethyl 8-(Phenylamino)-4,5-dihydro-1*H*-pyrazolo[4,3-*h*]quinazoline-3-carboxylate (7e). Compound **7d** (1.5 g, 2.66 mmol) in DCM (50 mL) was treated with trifluoroacetic acid (5 mL). The resulting mixture was stirred at room temperature for 1 h. DCM (40 mL) was added, and the organic phase was washed with saturated solution of sodium hydrogen carbonate, then with brine, dried over sodium sulfate, and concentrated. By crystallization from diisopropyl ether, the title compound was obtained (0.7 g, 80%). ^{1}H NMR (DMSO-d_6) δ ppm 1.33 (t, J = 7.1 Hz, 3H), 2.87 (t, J = 7.4 Hz, 2H), 2.99 (t, J = 7.4 Hz, 2H), 4.33 (q, J = 7.1 Hz, 2H), 6.90−6.95 (m, 1H), 7.25−7.30 (m, 2H), 7.85−7.90 (m, 2H), 8.40 (s, 1H), 9.53 (bs, 1H), 14.17 (bs, 1H). LCMS (ESI) m/z 336 $(M + H)^+$. HRMS (ESI) calcd for $C_{18}H_{17}N_5O_2 + H^+$ 336.1455, found 336.1454.

8-(Phenylamino)-1-(2,2,2-trifluoroethyl)-4,5-dihydro-1*H*-pyrazolo[4,3-*h*]quinazoline-3-carboxamide (1b). Compound **7b** (10.86 g, 26.04 mmol) was suspended in anhydrous EtOH (250 mL) and treated with 1.5 M KOH in 95% EtOH (60 mL, 90 mmol). The resulted suspension was refluxed for 2 h until an HPLC control revealed the disapparance of the starting material. The resulting precipitate was collected by filtration to give 10.68 g of potassium 1-methyl-8-(phenylamino)-4,5-dihydro-1*H*-pyrazolo[4,3-*h*]quinazoline-3-carboxylate (96%), which was used as such, without any purification. A suspension of this intermediate (197 mg, 0.46 mmol) in anhydrous DMF (5 mL) was treated with *N*,*N*-diisopropylethylamine (0.12 mL, 0.69 mmol), EDC (131 mg, 0.69 mmol) and HOBt·NH_3 (105 mg, 0.69 mmol). The reaction was kept at room temperature overnight and then was diluted with water and the resulting precipitate was collected by filtration to afford **1b** (148 mg, 78%). ^{1}H NMR (DMSO-d_6) δ ppm 2.85 (t, J = 8.0 Hz, 2H), 3.02 (t, J = 8.0 Hz, 2H), 5.79 (q, $^3J_{HF}$ = 8.9 Hz, 2H), 6.98−7.02 (m, 1H), 7.28−7.32 (m, 2H), 7.42 (bs, 1H), 7.46 (bs, 1H), 7.57−7.61 (m, 2H), 8.44 (s, 1H), 9.58 (bs, 1H). ^{13}C NMR (DMSO-d_6) δ ppm 163.2, 159.0, 157.4, 151.5, 143.3, 140.0, 137.2, 2 × 128.8, 124.9, 123.6 (q, $^1J_{CF}$ = 280 Hz), 121.7, 2 × 119.4, 118.6, 50.6, 23.6, 18.6. LCMS (ESI) m/z 389 $(M + H)^+$.

Compounds 1c and 1e. By employment of the above-described procedure, starting from **7c** and **7e**, the compounds **1c** and **1e** were prepared.

1-Phenyl-8-(phenylamino)-4,5-dihydro-1*H*-pyrazolo[4,3-*h*]-quinazoline-3-carboxamide (1c). Yield, 85%. ^{1}H NMR (DMSO-d_6) δ ppm 2.84−2.93 (m, 2H), 3.00−3.06 (m, 2H), 6.70−6.77 (m, 1H), 6.84−6.92 (m, 2H), 6.98−7.03 (m, 2H), 7.37 (bs, 1H), 7.50−7.63 (m, 5H), 7.63 (bs, 1H), 8.45 (s, 1H), 9.33 (s, 1H). ^{13}C NMR (DMSO-d_6) δ ppm 163.7, 158.8, 157.5, 151.9, 143.4, 140.6, 140.4, 137.4, 3 × 129.1, 2 × 128.3, 126.5, 2 × 125.2, 120.1, 118.9, 2 × 117.2, 28.9, 19.1. LCMS (ESI) m/z 383 $(M + H)^+$. HRMS (ESI) calcd for $C_{22}H_{18}N_6O + H^+$ 383.1615, found 383.1626.

8-(Phenylamino)-4,5-dihydro-1*H*-pyrazolo[4,3-*h*]quinazoline-3-carboxamide (1e). Yield, 56%. ^{1}H NMR (DMSO-d_6) δ ppm 2.84 (t, J = 8.0 Hz, 2H), 3.00 (t, J = 8.0 Hz, 2H), 6.93 (m, 1H), 7.25−7.34 (m, 2H), 7.34 (bs, 1H), 7.47 (bs, 1H), 7.85−7.90 (m, 2H), 8.38 (s, 1H), 13.91 (bs, 1H). ^{13}C NMR (DMSO-d_6) δ ppm 163.4, 159.7, 156.9, 152.9, 141.3, 140.8, 138.4, 2 × 128.3, 122.8, 120.8, 118.8, 2 × 118.2, 23.7, 18.9. HRMS (ESI) calcd for $C_{16}H_{14}N_6O + H^+$ 307.1302, found 307.1306.

1-Cyclohexyl-8-(phenylamino)-4,5-dihydro-1*H*-pyrazolo[4,3-*h*]-quinazoline-3-carboxamide (1f). A mixture of **1e** (46 mg, 0.15 mmol) in THF (4 mL) was treated with triphenylphosphine polimer-bound (0.2 g, 0.6 mmol), di-*tert*-butylazadicarboxylate (80 mg, 0.45 mmol), and cyclohexanol (60 μL, 0.6 mmol) for 1 h at room temperature. The resin was filtered off, and the solution was concentrated. Crystallization from diethyl ether gave the title compound (14 mg, 24%). ^{1}H NMR (DMSO-d_6) δ ppm 1.10−1.96 (m, 10H), 2.79 (t, J = 8.0 Hz, 2H), 2.97 (t, J = 8.0 Hz, 2H), 5.50−5.59 (m, 1H), 6.97−7.02 (m 1H), 7.23 (bs, 1H), 7.28−7.34 (m, 2H), 7.34 (bs, 1H), 7.61−7.65 (m, 2H), 8.40 (s, 1H), 9.42 (s, 1H). ^{13}C NMR (DMSO-d_6) δ ppm 164.1, 159.0, 157.0, 153.1, 140.8, 140.4, 135.3, 2 × 128.6, 124.3, 121.4, 2 × 119.2, 118.9, 57.8, 2 × 32.1, 3 × 24.3, 23.7, 18.3. LCMS (ESI) m/z 389 $(M + H)^+$.HRMS (ESI) calcd for $C_{22}H_{24}N_6O + H^+$ 389.2084, found 389.2084.

Compounds 1g−1i. By employment of the above-described procedure, starting from **1e** and using the suitable alcohol, the compounds **1g−1i** were prepared.

8-(Phenylamino)-1-(propan-2-yl)-4,5-dihydro-1*H*-pyrazolo[4,3-*h*]-quinazoline-3-carboxamide (1g). Yield, 48%. ^{1}H NMR (DMSO-d_6) δ ppm 1.48 (d, J = 6.6 Hz, 6H), 2.79 (t, J = 7.2 Hz, 2H), 2.97 (t, J = 7.2 Hz, 2H), 5.97 (m, 1H), 6.95−7.00 (m, 1H), 7.26 (bs, 1H), 7.31 (m, 2H), 7.36 (bs, 1H), 7.65−7.69 (m, 2H), 8.40 (s, 1H), 9.48 (s, 1H). LCMS (ESI) m/z 349 $(M + H)^+$. HRMS (ESI) calcd for $C_{19}H_{20}N_6O + H^+$ 349.1771, found 349.178.

1-(1-Methylpiperidin-4-yl)-8-(phenylamino)-4,5-dihydro-1*H*-pyrazolo[4,3-*h*]quinazoline-3-carboxamide (1h). Yield, 62%. ^{1}H NMR (DMSO-d_6) δ ppm 1.85−1.97 (m, 4H), 2.10−2.14 (m, 2H), 2.18 (s, 3H), 2.76−2.82 (m, 4H), 2.96 (t, J = 7.8 Hz, 2H), 5.43−5.54 (m, 1H), 7.00−7.03 (m, 1H), 7.25 (bs, 1H), 7.31−7.35 (m, 2H), 7.36 (bs, 1H), 7.59−7.61 (m, 2H), 8.40 (s, 1H), 9.42 (s, 1H). LCMS (ESI) m/z 404 $(M + H)^+$. HRMS (ESI) calcd for $C_{22}H_{25}N_7O + H^+$ 404.2193, found 404.2211.

8-(Phenylamino)-1-[2-(piperidin-1-yl)ethyl]-4,5-dihydro-1*H*-pyrazolo[4,3-*h*]quinazoline-3-carboxamide (1i). Yield, 60%. ^{1}H NMR (DMSO-d_6) δ ppm 1.20−1.26 (m, 6H), 2.18−2.24 (m, 4H), 2.62 (t, J = 6.6 Hz, 2H), 2.79 (t, J = 7.6 Hz, 2H), 2.97 (t, J = 7.6 Hz, 2H), 4.89 (t, J = 6.6 Hz, 2H), 6.94−6.99 (m, 1H), 7.25 (bs, 1H), 7.28−7.33 (m, 2H), 7.41 (bs, 1H), 7.63−7.67 (m, 2H),8.40 (s, 1H), 9.44 (s, 1H). ^{13}C NMR (DMSO-d_6) δ ppm 164.1, 159.2, 153.1, 156.8, 141.5, 140.8, 136.9, 2 × 128.1, 124.5, 121.1, 2 × 119.3, 118.8, 58.6, 2 × 53.8, 48.8, 2 × 25.4, 23.9, 23.7, 18.9. LCMS (ESI) m/z 418 $(M + H)^+$. HRMS (ESI) calcd for $C_{23}H_{27}N_7O + H^+$ 418.235, found 418.2363.

8-[(2-Acetylphenyl)amino]-1-methyl-4,5-dihydro-1*H*-pyrazolo-[4,3-*h*]quinazoline-3-carboxamide (22). Palladium acetate $Pd(OAc)_2$ (20 mg, 0.09 mmol), (±)-BINAP (55 mg, 0.09 mmol), and DMF (5 mL) were charged in a round-bottom flask flushed with argon. The flask was evacuated and backfilled with argon. The mixture was stirred under argon for 30 min and added to a mixture of **18**

(319 mg, 0.9 mmol), 2-acetylaniline (0.162 mL, 1.35 mmol), and potassium carbonate (1.24 g, 8.97 mmol) in DMF (10 mL). The resulting mixture was stirred at 80 °C for 4 h under argon. After cooling to room temperature, the reaction mixture was filtered on a pad of celite. The solvent was concentrated, the crude solid was purified by flash chromatography on silica gel (eluant, DCM/EtOH 90/10) to afford 153 mg (47%) of the title compound; mp 287 °C. ^{1}H NMR (DMSO-d_6) δ ppm 2.69 (s, 3H), 2.86 (t, J = 8.0 Hz, 2H), 3.01 (t, J = 8.0 Hz,, 2H), 4.34 (s, 3H), 7.09 (ddd, J = 8.0, 7.2, 1.1 Hz, 1H), 7.27 (bs, 1H), 7.49 (bs, 1H), 7.64 (ddd, J = 8.5, 7.2, 1.1 Hz, 1H), 8.07 (dd, J = 8.0, 1.1 Hz, 1H) 8.50 (s, 1H), 8.73 (dd, J = 8.5, 1.1 Hz, 1H), 11.59 (s, 1H). ^{13}C NMR (DMSO-d_6) δ ppm 203.1, 164.0, 158.2, 157.1, 153.2, 141.9, 141.0, 136.1, 134.7, 132.7, 124.8, 121.5, 120.8, 120.2, 118.7, 39.4, 28.7, 24.1, 18.7. LCMS (ESI) m/z 363 (M + H)$^+$. HRMS (ESI) calcd for $C_{19}H_{18}N_6O_2$ + H$^+$ 363.1564, found: 363.155.

Compounds 19−21, 23−49. By employment of the above-described procedure, starting from **18** and using the suitable substituted aniline, the compounds **19**−**21**, **23**−**49** were prepared.

1-Methyl-8-{[2-(trifluoromethyl)phenyl]amino}-4,5-dihydro-1*H*-pyrazolo[4,3-*h*]quinazoline-3-carboxamide (19). Yield, 10%. ^{1}H NMR (DMSO-d_6) δ ppm 2.79 (t, J = 7.2 Hz, 2H), 2.96 (t, J = 7.2 Hz, 2H), 4.03 (s, 3H), 7.22 (bs, 1H), 7.41 (t, J = 7.4 Hz, 1H), 7.43 (bs, 1H), 7.68 (t, J = 7.4 Hz, 1H), 7.74 (d, J = 7.4 Hz, 2H), 8.32 (s, 1H), 8.73 (s, 1H). ^{13}C NMR (DMSO-d_6) δ ppm 163.9, 160.5, 157.3, 152.9, 141.0, 137.9, 136.2, 132.9, 129.4, 126.5, 125.4, 124.4, 123.9 (q, $^1J_{CF}$ = 270 Hz, 120.0, 119.1, 38.2, 23.9, 18.8). LCMS (ESI) m/z 389 (M + H)$^+$. HRMS (ESI) calcd for $C_{18}H_{15}F_3N_6O$ + H$^+$ 389.1332, found 389.132.

1-Methyl-8-{[3-(trifluoromethyl)phenyl]amino}-4,5-dihydro-1*H*-pyrazolo[4,3-*h*]quinazoline-3-carboxamide (20). Yield, 25%. ^{1}H NMR (DMSO-d_6) δ ppm 2.84 (t, J = 7.2 Hz, 2H), 3.00 (t, J = 7.2 Hz, 2H), 4.32 (s, 3H), 7.26 (bs, 1H), 7.28 (d, J = 8.6 Hz, 1H), 7.46 (bs, 1H), 7.53 (t, J = 8.6 Hz, 1H), 7.92 (d, J = 8.6 Hz, 1H), 8.19 (s, 1H), 8.47 (s, 1H), 9.87 (s, 1H). ^{13}C NMR (DMSO-d_6) δ 163.9, 158.6, 156.7, 152.9, 141.6, 141.1, 136.4, 130.3, 129.3, 125.5 (q, $^1J_{CF}$ = 270 Hz), 124.9, 122.0, 119.9, 116.6, 114.2, 39.2, 24.1, 18.2. LCMS (ESI) m/z 389 (M + H)$^+$.

1-Methyl-8-{[4-(trifluoromethyl)phenyl]amino}-4,5-dihydro-1*H*-pyrazolo[4,3-*h*]quinazoline-3-carboxamide (21). Yield, 9.5%. ^{1}H NMR (DMSO-d_6) δ ppm 2.84 (t, J = 7.2 Hz, 2H), 3.00 (t, J = 7.2 Hz, 2H), 4.35 (s, 3H), 7.26 (bs, 1H), 7.48 (bs, 1H), 7.65 (m, 2H), 7.95 (m, 2H), 8.48 (s, 1H), 9.97 (s, 1H). ^{13}C NMR (DMSO-d_6) δ ppm 164.2, 158.9, 157.1, 153.3, 144.7, 141.3, 136.6, 2 × 125.7, 124.9, 124.5 (q, $^1J_{CF}$ = 270 Hz), 121.5, 120.5, 2 × 118.1, 39.8, 23.9, 18.6. LCMS (ESI) m/z 389 (M + H)$^+$. HRMS (ESI) calcd for $C_{18}H_{15}F_3N_6O$ + H$^+$ 389.1332, found 389.1317.

8-[(3-Acetylphenyl)amino]-1-methyl-4,5-dihydro-1*H*-pyrazolo-[4,3-*h*]quinazoline-3-carboxamide (23). Yield, 8%; ^{1}H NMR (DMSO-d_6) δ ppm 2.57 (s, 3H), 2.83 (t, J = 7.2 Hz, 2H), 2.99 (t, J = 7.2 Hz, 2H), 4.33 (s, 3H), 7.26 (bs, 1H), 7.46 (t, J = 7.8 Hz, 1H), 7.47 (bs, 1H), 7.59 (ddd, J = 7.8, 1.6, 1.0 Hz, 1H), 7.94 (ddd, J = 7.8, 2.2, 1.0 Hz, 1H), 8.32 (t, J = 2.2, 1.6 Hz, 1H), 8.44 (s, 1H), 9.73 (s, 1H). ^{13}C NMR (DMSO-d_6) δ ppm 198.3, 163.4, 158.8, 156.8, 153.0, 141.0, 140.9, 137.6, 136.3, 129.0, 124.6, 123.6, 121.7, 119.5, 118.0, 39.5, 26.7, 24.0, 18.9. LCMS (ESI) m/z 363 (M + H)$^+$. HRMS (ESI) calcd for $C_{19}H_{18}N_6O_2$ + H$^+$ 363.1564, found 363.1548.

8-[(4-Acetylphenyl)amino]-1-methyl-4,5-dihydro-1*H*-pyrazolo-[4,3-*h*]quinazoline-3-carboxamide (24). Yield, 8%. ^{1}H NMR (DMSO-d_6) δ ppm 2.52 (s, 3H), 2.85 (t, J = 7.4 Hz, 2H), 3.00 (t, J = 7.4 Hz, 2H), 4.37 (s, 3H), 7.26 (bs, 1H), 7.48 (bs, 1H), 7.85−7.90 (m, 2H), 7.91−7.95 (m, 2H), 8.49 (s, 1H), 9.99 (s, 1H). LCMS (ESI) m/z 363 (M + H)$^+$. HRMS (ESI) calcd for $C_{19}H_{18}N_6O_2$ + H$^+$ 363.1564, found 363.1559.

8-[(2-Methoxyphenyl)amino]-1-methyl-4,5-dihydro-1*H*-pyrazolo-[4,3-*h*]quinazoline-3-carboxamide (25). Yield, 77%; mp 256 °C. ^{1}H NMR (DMSO-d_6) δ ppm 2.81 (t, J = 7.7 Hz, 2H), 2.98 (t, J = 7.7 Hz, 2H), 3.85 (s, 3H), 4.25 (s, 3H), 6.92−6.99 (m, 1H), 7.00−7.09 (m, 2H), 7.24 (br s, 1H), 7.45 (br s, 1H), 8.01−8.05 (m, 1H), 8.13 (s, 1H), 8.38 (s, 1H). ^{13}C NMR (DMSO-d_6) δ 164.4, 159.6, 156.2, 153.4, 150.5, 141.4, 136.6, 129.2, 124.9, 122.3, 120.2, 119.6, 119.4, 110.0, 54.6, 38.5, 23.2, 18.0. LCMS (ESI) m/z 351 (M + H)$^+$.; HRMS (ESI) calcd for $C_{18}H_{18}N_6O_2$ + H$^+$ 351.1564, found 351.1559.

8-[(3-Methoxyphenyl)amino]-1-methyl-4,5-dihydro-1*H*-pyrazolo-[4,3-*h*]quinazoline-3-carboxamide (26). Yield, 25%; mp 298 °C. ^{1}H NMR (DMSO-d_6) δ ppm 2.81 (t, J = 7.4 Hz, 2H), 2.98 (t, J = 7.4 Hz, 2H), 3.74 (s, 3H), 4.34 (s, 3H), 6.54 (d, J = 8.3 Hz, 1H), 7.20 (dd, J = 8.3, 8.0 Hz, 1H), 7.25 (bs, 1H), 7.33 (d, J = 8.0 Hz, 1H), 7.35 (bs, 1H), 7.45 (bs, 1H), 8.41 (s, 1H), 9.48 (s, 1H). ^{13}C NMR (DMSO-d_6) δ ppm 164.7, 160.7, 159.7, 157.0, 153.8, 142.7, 141.8, 137.2, 125.5, 119.9, 129.3, 106.3, 104,9, 104.9, 54.8, 39.3, 23.5, 18.8. LCMS (ESI) m/z 351 (M + H)$^+$. HRMS (ESI) calcd for $C_{18}H_{18}N_6O_2$ + H$^+$ 351.1564, found 351.1566.

8-[(4-Methoxyphenyl)amino]-1-methyl-4,5-dihydro-1*H*-pyrazolo-[4,3-*h*]quinazoline-3-carboxamide (27). Yield, 62%; mp 234 °C. ^{1}H NMR (DMSO-d_6) δ ppm 2.79 (t, J = 7.2 Hz, 2H), 2.97 (t, J = 7.2 Hz, 2H), 3.73 (s, 3H), 4.30 (s, 3H), 6.87−6.91 (m, 2H), 7.25 (bs, 1H), 7.45 (s, 1H), 7.55−7.60 (m, 2H), 8.34 (s, 1H), 9.29 (s, 1H). ^{13}C NMR (DMSO-d_6) δ ppm 164.0, 159.2, 156.6, 154.4, 152.7, 140.9, 136.4, 133.4, 124.3 2 × 120.7, 118.1, 2 × 113.2, 54.9, 39.3, 23.8, 18.7. LCMS (ESI) m/z 351 (M + H)$^+$. HRMS (ESI) calcd for $C_{18}H_{18}N_6O_2$ + H$^+$ 351.1564, found 351.1557.

1-Methyl-8-[(2-nitrophenyl)amino]-4,5-dihydro-1*H*-pyrazolo-[4,3-*h*]quinazoline-3-carboxamide (28). Yield, 74%. ^{1}H NMR (DMSO-d_6) δ ppm 2.84 (t, J = 7.7 Hz, 2H), 3.00 (t, J = 7.70 Hz, 2H), 4.21 (s, 3 H), 7.25 (m, 1H), 7.27 (bs, 1H), 7.47 (bs, 1H), 7.73 (m, 1 H), 8.08 (m, 1H), 8.16 (m, 2H), 8.44 (s, 1H), 10.02 (s, 1 H). ^{13}C NMR (DMSO-d_6) δ ppm 163.9, 158.0, 156.9, 152.9, 140.9, 139.7, 135.9, 134.9, 134.3, 124.9, 124.6, 123.6, 122.3, 120.8, 39.0, 23.4, 18.5. LCMS (ESI) m/z 366 (M + H)$^+$. HRMS (ESI) calcd for $C_{17}H_{15}N_7O_3$ + H$^+$ 366.1309, found 366.1295.

1-Methyl-8-[(3-nitrophenyl)amino]-4,5-dihydro-1*H*-pyrazolo-[4,3-*h*]quinazoline-3-carboxamide (29). Yield, 64%. ^{1}H NMR (DMSO-d_6) δ ppm 2.85 (t, J = 7.6 Hz, 2H), 3.01 (t, J = 7.6 Hz, 2H), 4.36 (s, 3H), 7.27 (bs, 1H), 7.48 (bs, 1H), 7.59 (t, J = 8.2 Hz, 1H), 7.80 (dd, J = 8.2, 1.9 Hz, 1H), 8.02 (dd, J = 8.2, 1.0 Hz, 1H), 8.51 (s, 1H), 8.82 (dd, J = 1.9, 1.0 Hz, 1H), 10.08 (s, 1H). ^{13}C NMR (DMSO-d_6) δ ppm 163.8, 158.6, 156.8, 153.2, 148.4, 142.0, 140.8, 136.2, 129.3, 124.7, 123.8, 120.3, 115.0, 111.6, 39.2, 23.5, 18.3. LCMS (ESI) m/z 366 (M + H)$^+$. HRMS (ESI) calcd for $C_{17}H_{15}N_7O_3$ + H$^+$ 366.1309, found 366.1294.

1-Methyl-8-[(4-nitrophenyl)amino]-4,5-dihydro-1*H*-pyrazolo-[4,3-*h*]quinazoline-3-carboxamide (30). Yield, 63%. ^{1}H NMR (DMSO-d_6) δ ppm 2.87 (t, J = 7.3 Hz, 2H), 3.01 (t, J = 7.3 Hz, 2H), 4.37 (s, 3H), 7.30 (bs, 1H), 7.54 (bs, 1H), 7.97−8.00 (m, 2H), 7.22−7.25 (m, 2H), 8.54 (s, 1H), 10.39 (s, 1H). LCMS (ESI) m/z 366 (M + H)$^+$. HRMS (ESI) calcd for $C_{17}H_{15}N_7O_3$ + H$^+$ 366.1309, found 366.1303.

1-Methyl-8-[(2-methylphenyl)amino]-4,5-dihydro-1*H*-pyrazolo-[4,3-*h*]quinazoline-3-carboxamide (31). Yield, 7%. ^{1}H NMR (DMSO-d_6) δ ppm 2.24 (s, 3H), 2.78 (t, J = 7.3 Hz, 2H), 2.96 (t, J = 7.3 Hz, 2H), 4.11 (s, 3H), 7.05 (m, 1H), 7.17 (m, 1H), 7.21 (bs, 1H), 7.22 (bs, 1H), 7.22 (m, 1H), 7.42 (bs, 1H), 7.50 (m, 1H), 8.31 (s, 1H), 8.73 (s, 1H). LCMS (ESI) m/z 335 (M + H)$^+$. HRMS (ESI) calcd for $C_{18}H_{18}N_6O$ + H$^+$ 335.1615, found 335.1614.

1-Methyl-8-{[2-(methylsulfanyl)phenyl]amino}-4,5-dihydro-1*H*-pyrazolo[4,3-*h*]quinazoline-3-carboxamide (32). Yield, 52%; mp 215 °C. ^{1}H NMR (DMSO-d_6) δ ppm 2.39 (s, 3H), 2.79 (t, J = 7.3 Hz, 2H), 2.96 (t, J = 7.3 Hz, 2H), 4.12 (s, 3H), 7.15−7.25 (m, 2H), 7.22 (bs, 1H), 7.36−7.40 (m, 1H), 7.43 (bs, 1H), 7.60−7.63 (m, 1H), 8.32 (s, 1H), 8.63 (bs, 1H). ^{13}C NMR (DMSO-d_6) δ ppm 163.7, 159.8, 157.1, 152.9, 140.9, 137.5, 136.1, 133.3, 127.3, 125.3, 125.2, 125.2, 124.1, 118.4, 39.3, 23.8, 19.3, 15.1. LCMS (ESI) m/z 367 (M + H)$^+$. HRMS (ESI) calcd for $C_{18}H_{18}N_6OS$ + H$^+$ 367.1336, found 367.1346.

1-Methyl-8-{[2-(methylamino)phenyl]amino}-4,5-dihydro-1*H*-pyrazolo[4,3-*h*]quinazoline-3-carboxamide (33). Yield, 30%; mp 256 °C. ^{1}H NMR (DMSO-d_6) δ ppm 2.71 (d, J = 5 Hz, 3H), 2.76

(t, J = 7.8 Hz, 2H), 2.95 (t, J = 7.8 Hz, 2H), 4.09 (s, 3H), 5.05 (q, J = 5 Hz, 1H), 6.56−6.61 (m, 2H), 7.01−7.06 (m, 1H), 7.21 (bs, 1H), 7.24−7.27 (m, 1H), 7.42 (bs, 1H), 8.28 (s, 1H), 8.40 (s, 1H). ^{13}C NMR (DMSO-d_6) δ 164.1, 160.6, 156.7, 153.0, 144.8, 141.2, 136.6, 125.5, 125.5, 125.4, 124.2, 117.9, 114.9, 109.4, 38.7, 29.5, 23.7, 18.9. LCMS (ESI) m/z 350 (M + H)$^+$. HRMS (ESI) calcd for $C_{18}H_{19}N_7O$ + H$^+$ 350.1724, found: 350.1714.

8-[(2-Fluorophenyl)amino]-1-methyl-4,5-dihydro-1*H*-pyrazolo-[4,3-*h*]quinazoline-3-carboxamide (34). Yield, 13%. ^{1}H NMR (DMSO-d_6) δ ppm 2.80 (t, J = 7.2 Hz, 2H), 2.97 (t, J = 7.2 Hz, 2H), 4.16 (s, 3H), 7.10−7.27(m, 3H), 7.23 (bs, 1H), 7.44 (bs, 1H), 7.70−7.76 (m, 1H), 8.36 (s, 1H), 9.08 (bs, 1H). ^{13}C NMR (DMSO-d_6) δ 164.3, 159.6, 157.0, 155.8 (d, $^1J_{CF}$ = 160 Hz), 153.1, 141.2, 136.4, 128.0, 125.3, 124.6, 124.4, 123.7, 119.0, 115.1, 38.9, 23.8, 18.6. LCMS (ESI) m/z 339 (M + H)$^+$. HRMS (ESI) calcd for $C_{17}H_{15}FN_6O$ + H$^+$ 339.1364, found 339.1348.

1-Methyl-8-{[2-(propan-2-yl)phenyl]amino}-4,5-dihydro-1*H*-pyrazolo[4,3-*h*]quinazoline-3-carboxamide (35). Yield, 17%. ^{1}H NMR (DMSO-d_6) δ ppm 1.13 (d, J = 7.0 Hz, 6H), 2.76 (t, J = 7.8 Hz, 2H), 2.95 (t, J = 7.8 Hz, 2H), 3.25 (m, 1H), 4.05 (s, 3H), 7.15−7.22 (m, 2H), 7.20 (bs, 1H), 7.30−7.36 (m, 2H), 7.41 (bs, 1H), 8.26 (s, 1H), 8.74 (bs, 1H). ^{13}C NMR (DMSO-d_6) δ 163.8, 161.1, 157.1, 152.9, 144.3, 140.9, 136.9, 136.3, 127.3, 125.5, 125.5, 125.2, 124.2, 117.7, 38.7, 26.8, 23.8, 2 × 22.7, 18.7. LCMS (ESI) m/z 363 (M + H)$^+$. HRMS (ESI) calcd for $C_{20}H_{22}N_6O$ + H$^+$ 363.1928, found 363.1913.

Methyl 2-[(3-Carbamoyl-1-methyl-4,5-dihydro-1*H*-pyrazolo-[4,3-*h*]quinazolin-8-yl)amino]benzoate (36). Yield, 18%. ^{1}H NMR (DMSO-d_6) δ ppm 2.86 (t, J = 7.9 Hz, 2H), 3.01 (t, J = 7.9 Hz, 2H), 3.87 (s, 3H), 4.33 (s, 3H), 7.07 (dd, J = 8.7, 7.9 Hz, 1H), 7.27 (bs, 1H), 7.48 (bs, 1H), 7.64 (dd, J = 8.2, 7.9 Hz, 1H), 7.99 (d, J = 8.2 Hz, 1H), 8.50 (s, 1H), 8.67 (d, J = 8.7 Hz, 1H), 10.73 (s, 1H). LCMS (ESI) m/z 379 (M + H)$^+$. HRMS (ESI) calcd for $C_{19}H_{18}N_6O_3$ + H$^+$ 379.1513, found 379.1517.

8-[(2-Carbamoylphenyl)amino]-1-methyl-4,5-dihydro-1*H*-pyrazolo[4,3-*h*]quinazoline-3-carboxamide (37). Yield, 25%. ^{1}H NMR (DMSO-d_6) δ ppm 2.84 (t, J = 7.3 Hz, 2H), 3.00 (t, J = 7.3 Hz, 2H), 4.33 (s, 3H), 7.01 (m, 1H), 7.26 (bs, 1H), 7.47 (bs, 1H), 7.50 (m, 1H), 7.62 (bs, 1H), 7.78 (dd, J = 7.8, 1.5 Hz, 1H), 8.19 (bs, 1H), 8.45 (s, 1H), 8.61 (dd, J = 8.5, 0.7 Hz, 1H), 11.45 (s, 1H). ^{13}C NMR (DMSO-d_6) δ ppm 171.5, 163.8, 158.5, 156.8, 152.6, 141.3, 140.9, 136.1, 131.6, 128.7, 124.5, 119.9, 119.8, 119.0, 118.9, 39.4, 23.5, 17.4. LCMS (ESI) m/z 364 (M + H)$^+$. HRMS (ESI) calcd for $C_{18}H_{17}N_7O_2$ + H$^+$ 364.1516, found 364.1516.

1-Methyl-8-[(2-sulfamoylphenyl)amino]-4,5-dihydro-1*H*-pyrazolo[4,3-*h*]quinazoline-3-carboxamide (38). Yield, 22%. ^{1}H NMR (DMSO-d_6) δ ppm 2.86 (t, J = 7.3 Hz, 2H), 3.01 (t, J = 7.3 Hz, 2H), 4.29 (s, 3H), 7.14 (ddd, J = 8.0, 7.4, 1.0 Hz, 1H), 7.26 (bs, 1H), 7.48 (bs, 1H), 7.56 (ddd, J = 8.4, 7.4, 1.6 Hz, 1H), 7.84 (dd, J = 8.0, 1.6 Hz, 1H), 8.46 (dd, J = 8.4, 1.0 Hz, 1H), 8.48 (s, 1H). LCMS (ESI) m/z 400 (M + H)$^+$. HRMS (ESI) calcd for $C_{17}H_{17}N_7O_3S$ + H$^+$ 400.1186, found 400.1188.

8-(Biphenyl-2-ylamino)-1-methyl-4,5-dihydro-1*H*-pyrazolo[4,3-*h*]-quinazoline-3-carboxamide (39). Yield, 30%. ^{1}H NMR (DMSO-d_6) δ ppm 2.73 (t, J = 7.2 Hz, 2H), 2.93 (t, J = 7.2 Hz, 2H), 4.10 (s, 3H), 7.22 (bs, 1H), 7.23−7.43 (m, 9H), 7.71 (dd, J = 8.0, 1.1 Hz, 1H), 8.23 (s, 1H), 8.38 (bs, 1H). ^{13}C NMR (DMSO-d_6) δ ppm 163.9, 160.1, 157.2, 152.7, 141.1, 139.7, 137.0, 136.6, 136.4, 130.2, 2 × 128.8, 2 × 128.2, 128.2, 126.8, 126.1, 124.8, 124.3, 118.2, 38.9, 23.9, 18.5. LCMS (ESI) m/z 397 (M + H)$^+$. HRMS (ESI) calcd for $C_{23}H_{20}N_6O$ + H$^+$ 397.1771, found 397.1778.

1-Methyl-8-[(2-phenoxyphenyl)amino]-4,5-dihydro-1*H*-pyrazolo[4,3-*h*]quinazoline-3-carboxamide (40). Yield, 62%.; ^{1}H NMR (DMSO-d_6) δ ppm 2.79 (t, J = 7.3 Hz, 2H), 2.96 (t, J = 7.3 Hz, 2H), 4.23 (s, 3H), 6.93−6.99 (m, 3H), 7.06−7.11 (m, 2H), 7.18 (ddd, J = 8.0, 8.0, 1.6 Hz, 1H), 7.24 (bs, 1H), 7.31−7.36 (m, 2H), 7.44 (bs, 1H), 8.01 (dd, J = 7.9, 1.6 Hz, 1H), 8.33 (s, 1H), 8.50 (s, 1H). ^{13}C NMR (DMSO-d_6) δ 163.8, 158.7, 157.4, 157.1, 152.8, 147.8, 140.8, 135.9, 131.3, 2 × 130.3, 124.4, 124.0, 124.0, 123.9, 123.9, 119.5, 118.9, 2 × 118.1, 39.7, 24.3, 19.3. LCMS (ESI) m/z 413 (M + H)$^+$. HRMS (ESI) calcd for $C_{23}H_{20}N_6O_2$ + H$^+$ 413.172, found 413.1711.

8-[(2-Benzylphenyl)amino]-1-methyl-4,5-dihydro-1*H*-pyrazolo-[4,3-*h*]quinazoline-3-carboxamide (41). Yield, 33%. ^{1}H NMR (DMSO-d_6) δ ppm 2.76 (t, J = 7.3 Hz, 2H), 2.95 (t, J = 7.3 Hz, 2H), 4.02 (s, 2H), 4.06 (s, 3H), 7.07−7.25 (m, 9H), 7.42 (bs, 1H), 7.53 (dd, J = 7.9, 0.8 Hz, 1H), 8.28 (s, 1H), 8.69 (bs, 1H). LCMS (ESI) m/z 411 (M + H)$^+$. HRMS (ESI) calcd for $C_{24}H_{22}N_6O$ + H$^+$ 411.1928, found 411.1931.

1-Methyl-8-{[2-(phenylamino)phenyl]amino}-4,5-dihydro-1*H*-pyrazolo[4,3-*h*]quinazoline-3-carboxamide (42). Yield, 22%. ^{1}H NMR (DMSO-d_6) δ ppm 2.79 (t, J = 7.3 Hz, 2H), 2.97 (t, J = 7.3 Hz, 2H), 4.21 (s, 3H), 6.73−6.78 (m, 1H), 6.85−6.90 (m, 2H), 6.99−7.07 (m, 2H), 7.13−7.19 (m, 2H), 7.23 (bs, 1H), 7.25−7.28 (m, 1H), 7.44 (bs, 1H), 7.82−7.87 (m, 1H), 8.35 (s, 1H), 8.44 (bs, 1H). ^{13}C NMR (DMSO-d_6) δ 163.6, 159.4, 156.8, 152.8, 144.5, 140.8, 136.2, 135.0, 131.8, 2 × 128.8, 124.3, 124.1, 123.9, 122.0, 120.6, 118.9, 118.5, 2 × 115.9, 39.0, 23.8, 18.7. LCMS (ESI) m/z 412 (M + H)$^+$. HRMS (ESI) calcd for $C_{23}H_{21}N_7O$ + H$^+$ 412.188, found: 412.1867.

1-Methyl-8-{[2-(phenylcarbonyl)phenyl]amino}-4,5-dihydro-1*H*-pyrazolo[4,3-*h*]quinazoline-3-carboxamide (43). Yield, 55%. ^{1}H NMR (DMSO-d_6) δ ppm 2.79 (t, J = 7.3 Hz, 2H), 2.98 (t, J = 7.3 Hz, 2H), 4.26 (s, 3H), 7.14 (ddd, J = 8.4, 7.8, 1.1 Hz, 1H), 7.26 (bs, 1H), 7.45−7.66 (m, 8H), 8.23 (dd, J = 8.4, 0.7 Hz, 1H), 8.27 (s, 1H), 10.27 (s, 1H). LCMS (ESI) m/z 425 (M + H)$^+$. HRMS (ESI) calcd for $C_{24}H_{20}N_6O_2$ + H$^+$ 425.172, found 425.1715.

1-Methyl-8-{[2-(phenylsulfanyl)phenyl]amino}-4,5-dihydro-1*H*-pyrazolo[4,3-*h*]quinazoline-3-carboxamide (44). Yield, 44%. ^{1}H NMR (DMSO-d_6) δ ppm 2.80 (t, J = 7.3 Hz, 2H), 2.97 (t, J = 7.3 Hz, 2H), 4.18 (s, 3H), 7.13 (td, J = 7.8, 1.5 Hz, 1H), 7.18−7.23 (m, 3H), 7.24 (bs, 1H), 7.26−7.32 (m, 2H), 7.41−7.45 (m, 2H), 7.46 (bs, 1H), 8.00 (dd, J = 8.7, 1.5 Hz, 1H), 8.35 (s, 1H), 8.64 (s, 1H). ^{13}C NMR (DMSO-d_6) δ 163.8, 159.1, 156.9, 153.1, 141.0, 140.6, 136.1, 135.7, 134.1, 2 × 129.4, 129.1, 2 × 128.7, 126.7, 125.7, 124.5, 124.4, 123.2, 119.5, 39.1, 23.9, 18.6. LCMS (ESI) m/z 429 (M + H)$^+$. HRMS (ESI) calcd for $C_{23}H_{20}N_6OS$ + H$^+$ 429.1492, found 429.1505.

8-{[2-Acetyl-3-(4-methylpiperazin-1-yl)phenyl]amino}-1-methyl-4,5-dihydro-1*H*-pyrazolo[4,3-*h*]quinazoline-3-carboxamide (45). Yield, 36%. ^{1}H NMR (DMSO-d_6) δ ppm 2.22 (s, 3H), 2.40−2.48 (m, 4H), 2.56 (s, 3H), 2.80 (t, J = 7.3 Hz, 2H), 2.89−2.94 (m, 4H), 2.97 (t, J = 7.3 Hz, 2H), 4.22 (s, 3H), 6.94 (d, J = 8.8 Hz, 1H), 7.24 (bs, 1H), 7.39 (dd, J = 8.8, 7.8 Hz), 7.45 (bs, 1H), 7.70 (d, J = 7.8 Hz, 1H), 8.35 (s, 1H), 9.03 (s, 1H). ^{13}C NMR (DMSO-d_6) δ ppm 206.2, 164.7, 158.9, 156.7, 153.3, 152.1, 141.1, 137.2, 136.2, 130.7, 127.7, 124.6, 119.5, 117.8, 114.1, 2 × 54.5, 2 × 52.5, 45.4, 39.2, 30.9, 24.1, 18.8. LCMS (ESI) m/z 461 (M + H)$^+$. HRMS (ESI) calcd for $C_{24}H_{28}N_8O_2$ + H$^+$ 461.2408, found 461.2417.

8-{[2-Acetyl-4-(4-methylpiperazin-1-yl)phenyl]amino}-1-methyl-4,5-dihydro-1*H*-pyrazolo[4,3-*h*]quinazoline-3-carboxamide (46). Yield, 50%; mp 242 °C. ^{1}H NMR (DMSO-d_6) δ ppm 2.26 (s, 3H), 2.47−2.55 (signal obscured by DMSO, 4H), 2.65 (s, 3H), 2.82 (t, J = 7.7 Hz, 2H), 2.99 (t, J = 7.7 Hz, 2H), 3.12−3.19 (m, 4H), 4.31 (s, 3H), 7.25 (br s, 1H), 7.32 (dd, J = 9.1, 2.7 Hz, 1H), 7.43 (d, J = 2.7 Hz, 1H), 7.47 (bs, 1H), 8.42 (s, 1H), 8.48 (d, J = 9.1 Hz, 1H), 11.03 (s, 1H). ^{13}C NMR (DMSO-d_6) δ ppm 203.2, 163.9, 158.2, 157.0, 153.2, 145.3, 140.7, 136.3, 133.8, 124.6, 123.4, 122.5, 120.6, 119.9, 117.8, 2 × 54.5, 2 × 48.4, 45.7, 39.3, 28.6, 24.0, 18.6. LCMS (ESI) m/z 461 (M + H)$^+$. HRMS (ESI) calcd for $C_{24}H_{28}N_8O_2$ + H$^+$ 461.2408, found 461.2411.

8-{[2-Acetyl-5-(4-methylpiperazin-1-yl)phenyl]amino}-1-methyl-4,5-dihydro-1*H*-pyrazolo[4,3-*h*]quinazoline-3-carboxamide (47). Yield, 45%. ^{1}H NMR (DMSO-d_6) δ ppm 2.23 (s, 3H), 2.42−2.47 (m, 4H), 2.54 (s, 3H), 2.85 (t, J = 7.3 Hz, 2H), 3.00 (t, J = 7.7 Hz, 2H), 3.35−3.40 (m, 4H), 4.33 (s, 3H), 6.60 (dd, J = 9.1, 2.7 Hz, 1H), 7.27 (bs, 1H), 7.48 (bs, 1H), 7.85 (d, J = 9.1 Hz, 1H), 8.30 (d, J = 2.7 Hz, 1H), 8.52 (s, 1H), 12.12 (s, 1H). ^{13}C NMR (DMSO-$_{d6}$) δ ppm 200.0, 164.8, 158.4, 156.1, 155.1, 153.6, 144.4, 141.1, 136.2, 133.9, 125.3, 120.7, 111.9, 105.4,

100.6, 2 × 54.2, 2 × 46.0, 45.3, 38.9, 27.4, 24.0, 18.2. LCMS (ESI) m/z 461 $(M + H)^+$. HRMS (ESI) calcd for $C_{24}H_{28}N_8O_2 + H^+$ 461.2408, found 461.2394.

8-{[2-Methoxy-4-(4-methylpiperazin-1-yl)phenyl]amino}-1-methyl-4,5-dihydro-1*H*-pyrazolo[4,3-*h*]quinazoline-3-carboxamide (48). Yield, 11%; mp 127 °C. ^{1}H NMR (DMSO-d_6) δ ppm 2.30 (br s, 3H), 2.52−2.62 (m, 4H), 2.77 (t, J = 7.7 Hz, 2H), 2.96 t, J = 7.7 Hz, 2H), 3.10−3.20 (m, 4H), 3.80 (s, 3H), 4.22 (s, 3H), 6.50 (dd, J = 8.8, 2.5 Hz, 1H), 6.63 (d, J = 2.5 Hz, 1H), 7.23 (br s, 1H), 7.43 (s, 1H), 7.65 (d, J = 8.8 Hz, 1H), 8.00 (s, 1H), 8.28 (s, 1H). ^{13}C NMR (DMSO-d_6) δ ppm 164.9, 160.0, 157.1, 153.3, 152.4, 149.0, 141.4, 136.8, 124.9, 123.7, 121.0, 118.4, 106.3, 100.0, 55.7, 2 × 54.5, 2 × 48.9, 45.8, 39.2, 24.3, 18.9. LCMS (ESI) m/z 449 $(M + H)^+$. HRMS (ESI) calcd for $C_{23}H_{28}N_8O_2 + H^+$ 449.2408, found 449.2398.

8-{[2-Methoxy-5-(4-methylpiperazin-1-yl)phenyl]amino}-1-methyl-4,5-dihydro-1*H*-pyrazolo[4,3-*h*]quinazoline-3-carboxamide (49). Yield, 25%; mp 133 °C. ^{1}H NMR (DMSO-d_6) δ ppm 2.22 (s, 3H), 2.43−2.49 (m, 4H), 2.80 (t, J = 7.7 Hz, 2H), 2.98 (t, J = 7.7 Hz, 2H), 2.99−3.03 (m, 4H), 3.78 (s, 3H), 4.26 (s, 3H), 6.58 (dd, J = 8.9, 2.9 Hz, 1H), 6.91 (d, J = 8.9 Hz, 1H), 7.25 (bs., 1H), 7.45 (bs, 1H), 7.72 (d, J = 2.9 Hz, 1H), 8.06 (s, 1H), 8.39 (s, 1H). ^{13}C NMR (DMSO-d_6) δ ppm 163.6, 158.9, 157.2, 152.9, 145.7, 143.8, 140.9, 136.1, 129.0, 124.4, 118.9, 111.3, 110.7, 110.1, 56.2, 2 × 54.7, 2 × 49.9, 45.9, 39.2, 23.8, 18.8. LCMS (ESI) m/z 449 $(M + H)^+$. HRMS (ESI) calcd for $C_{23}H_{28}N_8O_2 + H^+$ 449.2408, found 449.24.

Ethyl 8-({2-[(*tert*-Butoxycarbonyl)amino]phenyl}amino)-1-methyl-4,5-dihydro-1*H*-pyrazolo[4,3-*h*]quinazoline-3-carboxylate (77). Palladium acetate [$Pd(OAc)_2$] (101 mg, 0.45 mmol), (±)-BINAP (280 mg, 0.45 mmol), and DMF (65 mL) were charged to a round-bottom flask flushed with argon. The flask was evacuated and backfilled with argon. The mixture was stirred under argon for 30 min and added to a mixture of *N*-Boc-*o*-phenylendiamine (2.6 g, 12.52 mmol), compound **16** (1.6 g, 4.16 mmol), and potassium carbonate (5.74 g, 41.53 mmol) in DMF (50 mL). The resulting mixture was stirred at 70 °C for 6 h under argon. After cooling to room temperature, the reaction mixture was filtered on a pad of celite. The solvent was concentrated, the crude solid was purified by flash chromatography on silica gel (eluant, hexane/ethyl acetate 60/40) to afford the title compound (1.18 g, 61%). ^{1}H NMR (DMSO-d_6) δ ppm 1.30 (t, J = 7.1 Hz, 3H), 1.44 (s, 9H), 2.83 (t, J = 7.3 Hz, 2H), 2.96 (t, J = 7.7 Hz, 2H), 4.18 (s, 3H), 4.28 (q, J = 7.7 Hz, 2H), 7.06−7.15 (m, 2 H), 7.47−7.52 (m, 1H), 7.68−7.71 (m, 1H), 8.36 (s, 1H), 8.64 (s, 1H), 8.68 (bs, 1H). LCMS (ESI) m/z 465 $(M + H)^+$. HRMS (ESI) calcd for $C_{24}H_{28}N_6O_4 + H^+$ 465.2245, found 465.2238.

Ethyl 8-[(2-aminophenyl)amino]-1-methyl-4,5-dihydro-1*H*-pyrazolo[4,3-*h*]quinazoline-3-carboxylate (78). To a solution of **77** (0.85 g, 1.83 mmol) in DCM (50 mL) HCl 4 N in dioxane (30 mL) was added. The solution was stirred at room temperature for 2 h and then the solvent removed in vacuo. The residue was crystallized from diethyl ether to give compound **78** (0.70 g, 96%) of the title compound. ^{1}H NMR (DMSO-d_6) δ ppm (as free base) 1.30 (t, J = 7.1 Hz, 3H), 2.80 (t, J = 7.3 Hz, 2H), 2.95 (t, J = 7.7 Hz, 2H), 4.17 (s, 3 H), 4.28 (q, J = 7.1 Hz, 2 H), 4.83 (bs, 2 H), 6.56 (td, J = 7.9, 1.5 Hz, 1H), 6.74 (dd, J = 7.9, 1.5 Hz, 1H), 6.88 (td, J = 7.9, 1.5 Hz, 1H), 7.30 (dd, J = 7.9, 1.5 Hz, 1H), 8.31 (s, 1H), 8.51 (s, 1H). LCMS (ESI) m/z 365 $(M + H)^+$. HRMS (ESI) calcd for $C_{19}H_{20}N_6O_2 + H^+$ 365.172, found 365.1713.

Ethyl 8-{[2-(Acetylamino)phenyl]amino}-1-methyl-4,5-dihydro-1*H*-pyrazolo[4,3-*h*]quinazoline-3-carboxylate (79). To a solution of **78** (0.3 g, 0.75 mmol) and DIPEA (0.51 mL, 2.93 mmol) in DCM (30 mL) under nitrogen acetyl chloride (0.11 mL, 1.49 mmol) dissolved in DCM (2 mL) was added. After 1 h the reaction mixture was concentrated and the residue was diluted with DCM, washed with $NaHCO_3$ (2 × 30 mL) and water (1 × 20 mL), dried over anhydrous Na_2SO_4, and concentrated. The crude residue was diluted with diethyl ether and decanted, to give 0.22 g (72%) of the final compound. ^{1}H NMR (DMSO-d_6) δ ppm 1.30 (t, J = 7.1 Hz, 3H), 2.07 (s, 3H), 2.83 (t, J = 7.4 Hz, 2H), 2.96 (t, J = 7.4 Hz, 2H), 4.18 (s, 3H), 4.28 (q, J = 7.1 Hz, 1H), 7.05−7.11 (m, 1H), 7.14−7.20 (m, 1H), 7.48 (d, J = 7.7 Hz, 1H), 7.77 (d, J = 7.7 Hz, 1H), 8.37 (s, 1 H), 8.58 (bs, 1H), 9.62 (bs, 1 H). HRMS (ESI) calcd for $C_{21}H_{22}N_6O_3 + H^+$ 336.1567, found: 336.1582.

8-[(2-Aminophenyl)amino]-1-methyl-4,5-dihydro-1*H*-pyrazolo-[4,3-*h*]quinazoline-3-carboxamide (80). To a suspension of **78** (65 mg, 0.18 mmol) in EtOH (10 mL) 30% NH_4OH (20 mL) was added. The mixture was maintained at 70 °C under stirring for 12 h in a sealed bottle. The solvent was then evaporated to dryness and the crude was purified by reverse phase chromatography to give **80** (10 mg, 17%) of the final compound. ^{1}H NMR (DMSO-d_6) δ ppm 2.7 (t, J = 7.3 Hz, 2H), 2.96 (t, J = 7.7 Hz, 2H), 4.15 (s, 3H), 4.84 (bs, 2H), 6.57 (td, J = 7.9, 1.5 Hz, 1H), 6.74 (dd, J = 7.9, 1.5 Hz, 1H), 6.88 (td, J = 7.9, 1.5 Hz, 1H), 7.21 (bs, 1 H), 7.32 (dd, J = 7.9, 1.5 Hz, 1H), 7.42 (bs, 1H), 8.29 (s, 1H), 8.47 (s, 1H). ^{13}C NMR (DMSO-d_6) δ 164.2, 160.3, 155.9, 153.3, 142.7, 140.9, 136.5, 125.3, 125.2, 125.1, 124.4, 124.2, 117.9, 115.7, 38.3, 23.8, 18.7. LCMS (ESI) m/z 336 $(M + H)^+$. HRMS (ESI) calcd for $C_{17}H_{17}N_7O + H^+$ 336.1567, found 336.1582.

8-{[2-(Acetylamino)phenyl]amino}-1-methyl-4,5-dihydro-1*H*-pyrazolo[4,3-*h*]quinazoline-3-carboxamide (81). By employment of the above-described procedure, starting from **79**, the compound **81** was prepared. Yield, 64%. ^{1}H NMR (DMSO-d_6) δ ppm: 2.07 (s, 3H), 2.83 (t, J = 7.4 Hz, 2H), 2.97 (t, J = 7.4 Hz, 2H), 4.16 (s, 3H), 7.06−7.12 (m, 1H), 7.14−7.20 (m, 1H), 7.23 (bs, 1H), 7.44 (bs, 1H), 7.47 (dd, J = 8.2, 1.2 Hz, 1H), 7.80 (dd, J = 7.9, 1.2 Hz, 1H), 8.35 (s, 1H), 8.56 (bs, 1 H), 9.62 (bs, 1H). LCMS (ESI) m/z 378 $(M + H)^+$. HRMS (ESI) calcd for $C_{19}H_{19}N_7O_2 + H^+$ 378.1673, found: 378.1679.

***N*-(4-Bromo-2-methoxyphenyl)acetamide (83a).** A mixture of 4-bromo-2-methoxy-phenylamine **82a** (2.00 g, 9.90 mmol) in acetic anhydride (2 mL, 21.15 mmol) was stirred at room temperature overnight. The solvent was evaporated to dryness, and the solid was tritured with diethyl ether and filtered to give the title compound (1.26 g, 51%). ^{1}H NMR (DMSO-d_6) δ ppm 2.07 (s, 3H), 3.84 (s, 3H), 7.07 (dd, J = 8.5, 2.2 Hz, 1H), 7.20 (d, J = 2.2 Hz, 1H), 7.89 (d, J = 8.5 Hz, 1H), 9.17 (bs, 1H). LCMS (ESI) m/z 245 $(M + H)^+$.

***N*-(2-Acetyl-4-bromophenyl)acetamide (83b).** By employment of the above-described procedure, starting from **82b**, the compound **83b** was prepared. Yield, 42%. ^{1}H NMR (DMSO-d_6) δ ppm 2.10 (s, 3H), 2.60 (s, 3H), 7.75 (dd, J = 8.9, 2.4 Hz, 1H), 8.04 (d, J = 2.4 Hz, 1H), 8.11 (d, J = 8.9 Hz, 1H), 10.94 (s, 1 H). LCMS (ESI) m/z 257 $(M + H)^+$.

***N*-[2-Methoxy-4-(4-methylpiperazin-1-yl)phenyl]acetamide (84a).** $Pd_2(dba)_3$ (47 mg, 0.05 mmol), 2-dicyclohexylphosphino-2′-(*N*,*N*-dimethylamino)-biphenyl (39 mg, 0.02 mmol), and **83a** (1.26 g, 5.16 mmol) in THF (5 mL) were charged in a round-bottom flask flushed with argon. The flask was evacuated and backfilled with argon. $LiN(TMS)_2$ solution (1 M in THF, 11.5 mL) and 4-methylpiperazine (0.67 mL, 6.2 mmol) were added, and the reaction refluxed for 3 h. The reaction mixture was then allowed to cool to room temperature and concentrated. The crude solid was purified by flash chromatography on silica gel (eluant, DCM/MeOH 90/10) to afford compound **84a** (1.26 g, 91%). ^{1}H NMR (DMSO-d_6) δ ppm 2.01 (s, 3H), 2.26 (bs, 3H), 2.46−2.54 (signal oscured by DMSO, 4H), 3.07−3.15 (m, 4H), 3.80 (s, 3H), 6.42 (dd, J = 8.7, 2.5 Hz, 1H), 6.58 (d, J = 2.5 Hz, 1H), 7.58 (d, J = 8.66, 1H), 8.88 (s, 1H). LCMS (ESI) m/z 264 $(M + H)^+$.

***N*-[2-Acetyl-4-(4-methylpiperazin-1-yl)phenyl]acetamide (84b).** By employment of the above-described procedure, starting from **83b**, the compound **84b** was prepared. Yield, 53%. ^{1}H NMR (DMSO-d_6) δ ppm 2.10 (s, 3H), 2.27 (s, 3H), 2.60 (s, 3H), 2.43−2.57 (m, 4H), 3.07−3.17 (m, 4H), 7.11 (dd, J = 8.7, 2.6 Hz, 1H), 7.43 (d, J = 2.6 Hz, 1H), 7.82 (d, J = 8.7 Hz, 1H), 10.94 (s, 1H). LCMS (ESI) m/z 276 $(M + H)^+$.

1-(4-Methoxy-3-nitrophenyl)-4-methylpiperazine (84c). $Pd(OAc)_2$ (85 mg, 0.38 mmol), 2-dicyclohexylphosphino-2′-(*N*,*N*-dimethylamino)-biphenyl (225 mg, 0.57 mmol), K_3PO_4 (2.26 g, 10.68 mmol),

and 4-bromo-1-methoxy-2-nitro-benzene **83c** (1.77 g, 7.63 mmol) in THF (50 mL) were charged in a round-bottom flask flushed with argon. The flask was evacuated and backfilled with argon. 4-Methylpiperazine (1.0 mL, 9.15 mmol) was added, and the reaction mixture was refluxed for 72 h. The reaction mixture was then allowed to cool to room temperature and concentrated. The crude solid was purified by flash chromatography on silica gel (eluant, DCM/EtOH 90/10) to afford the title compound (1.0 g, 55%). ^{1}H NMR (DMSO-d_6) δ ppm 2.22 (s, 3H), 2.42−2.48 (m, 4H), 3.07−3−13 (m, 4H), 3.83 (s, 3H), 7.22 (part of ABX sytem, J = 9.3 Hz, 1H), 7.26 (part of ABX sytem, J = 9.3, 2.9 Hz, 1H), 7.35 (d, J = 2.9 Hz, 1H). LCMS (ESI) m/z 252 $(M + H)^+$. HRMS (ESI) calcd for $C_{12}H_{17}N_3O_3 + H^+$ 252.1343, found 252.1342.

1-[2-(4-Methylpiperazin-1-yl)-6-nitrophenyl]ethanone (84d). In a sealed tube, 1-(2-chloro-6-nitro-phenyl)-ethanone **83d** (300 mg, 1.5 mmol) and 4-methylpiperazine (12.0 mL) were heated for 40 h at 120 °C. The solvent was removed under reduced pressure, and the residue was dissolved in DCM. The solution was washed twice with water, and the organic phase was dried over anhydrous sodium sulfate. The crude was purified by flash chromatography (eluant, acetone/MeOH 75:25), affording **84** (272 mg, 68%). ^{1}H NMR (DMSO-d_6) δ ppm 2.21 (s, 3H), 2.35−2.44 (m, 4H), 2.86−2.91 (m, 4H), 7.66 (t, J = 8.7 Hz, 1H), 7.76 (dd, J = 8.7, 0.8 Hz, 1H), 7.91 (dd, J = 8.7, 0.8 Hz, 1H). LCMS (ESI) m/z 264 $(M + H)^+$. HRMS (ESI) calcd for $C_{13}H_{17}N_3O_3 + H^+$ 264.1343, found 264.133.

2-Methoxy-4-(4-methylpiperazin-1-yl)aniline (85a). A solution of **84a** (2.3 g, 8.73 mmol) in EtOH (52 mL) was treated with HCl 37% (26 mL). After 1 h under reflux, the mixture was concentrated and triturated with hexane to give in quantitative yield, 2.5 g of the title compound as dihydrochloride salt. ^{1}H NMR (DMSO-d_6) δ ppm 2.82 (bs, 3H), 3.08−3.16 (m, 4 H), 3.46−3.53 (m, 2H), 3.85−3.92 (m, 2H), 3.90 (s, 3H), 6.60 (dd, J = 8.8, 2.6 Hz, 1H), 6.78 (d, J = 2.6 Hz, 1H), 7.25 (d, J = 8.8 Hz, 1H), 9.74 (bs, 3H) 10.79 (bs, 1H). LCMS (ESI) m/z 222 $(M + H)^+$. HRMS (ESI) calcd for $C_{12}H_{19}N_3O + H^+$ 222.1601, found 222.1596.

1-[2-Amino-4-(4-methylpiperazin-1-yl)phenyl]ethanone (85b). By employment of the above-described procedure, starting from **84b**, the compound **85b** was prepared. Yield, 45%. ^{1}H NMR (DMSO-d_6) δ ppm 2.53 (s, 3H), 2.82 (bs, 3H), 2.92−3.03 (m, 4H), 3.08−3.25 (m, 4H), 3.58−3.66 (m, 4H), 6.85 (d, J = 8.5 Hz, 1H), 7.15 (dd, J = 8.5, 2.5 Hz, 1H), 7.27 (d, J = 2.5 Hz, 1H), 10.40 (bs, 1H). LCMS (ESI) m/z 234 $(M + H)^+$. HRMS (ESI) calcd for $C_{13}H_{19}N_3O + H^+$ 234.1601, found 234.1602.

2-Methoxy-5-(4-methylpiperazin-1-yl)aniline (85c). A solution of **84c** (1.0 g, 3.97 mmol) in MeOH (100 mL) in the presence of Pd/C 10% (150 mg) was hydrogenated at 35 psi for 2 h. The mixture was filtered over a pad of celite, and the solution was concentrated to afford the title compound (0.8 g, 90%). ^{1}H NMR (DMSO-d_6) δ ppm 2.20 (s, 3H), 2.39−2.43 (m, 4H), 2.91−2.96 (m, 4H), 3.67 (s, 3H), 4.54 (bs, 2H), 6.08 (dd, J = 8.7, 2.9 Hz, 1H), 6.29 (d, J = 2.9 Hz, 1H), 6.63 (d, J = 8.7 Hz, 1H). LCMS (ESI) m/z 222 $(M + H)^+$. HRMS (ESI) calcd for $C_{12}H_{19}N_3O + H^+$ 222.1601, found 222.1609.

1-[2-Amino-6-(4-methylpiperazin-1-yl)phenyl]ethanone (85d). To a solution of **84d** (0.270 g, 1.02 mmol) in a mixture (1:1:1.5:2.5) of cyclohexene:THF:H_2O:EtOH (12 mL), Pd/C 10% (328 mg), and two drops of HCl 37% were added. The mixture was heated at 70 °C for 3 h. The Pd was filtered over a pad of celite, and the solvents were removed from the filtrate under reduced pressure. The crude was purified by flash chromatography (eluant, DCM/MeOH/7 N NH_3 in MeOH 9/1/1), to give compound **85d** as orange oil (225 mg, 95%). ^{1}H NMR (DMSO-d_6) δ ppm 2.51 (s, 3H), 2.84 (bs, 3H), 2.94−3.05 (m, 2H), 3.13−3.23 (m, 4H), 3.41−3.49 (m, 2H), 6.32 (dd, J = 7.9, 0.8 Hz, 1H), 6.49 (dd, J = 8.3, 0.8 Hz, 1H), 7.09 (dd, dd, J = 8.3, 7.9 Hz, 1H), 9.95 (bs, 1H). LCMS (ESI) m/z 234 $(M + H)^+$. HRMS (ESI) calcd for $C_{13}H_{19}N_3O + H^+$ 234.1601, found 234.1605.

1-[2-Hydroxy-4-(4-methylpiperazin-1-yl)phenyl]ethanone (87). 1-(4-Fluoro-2-hydroxy-phenyl)-ethanone **86** (4.5 g, 29.22 mmol) was treated with 4-methylpiperazine (5 mL) at 130 °C for 3 h. The solvent was evaporated under vacuum to yield give 6.7 g of the desired compound in a quantitative yield. ^{1}H NMR (DMSO-d_6) δ ppm 2.20 (s, 3H), 2.37−2.41 (m, 4H), 2.47 (s, 3H), 3.33−3.38 (m, 4H), 6.26 (d, J = 2.6 Hz, 1H), 6.52 (dd, J = 9.1, 2.6 Hz, 1H), 7.66 (d, J = 9.1 Hz, 1H), 12.73 (s, 1H). LCMS (ESI) m/z 235 $(M + H)^+$. HRMS (ESI) calcd for $C_{13}H_{18}N_2O_2 + H^+$ 235.1441, found 235.1431.

1-[2-Amino-4-(4-methyl-piperazin-1-yl)-phenyl]-ethanone (85e). To a solution of **87** (5.2 g, 22.20 mmol) in DMA (50 mL), NaOH (2.7 g, 67.50 mmol) was added. The mixture was stirred at room temperature for 1 h, then 2-bromo-2-methylpropanamide (11.1 g, 66.7 mmol) was added and the mixture was stirred at room temperature overnight. NaOH (8.01 g, 200 mmol) was added, and the resulting mixture was stirred at 100 °C for 2 h, then water (50 mL) was added, and the mixture was stirred at 100 °C for 1 h. After cooling to room temperature, the mixture was concentrated, diluted with DCM, and washed with water. The organic phase was dried over sodium sulfate, the solvent allowed under reduced pressure, and the crude solid was purified by flash chromatography on silica gel (eluant: DCM/EtOH, 95/5) to afford **85e** (1.51 g, 30%). ^{1}H NMR (DMSO-d_6) δ ppm 2.21 (s, 3H), 2.36 (s, 3H), 2.37−2.43 (m, 4H), 3.19−3.25 (m, 4H), 6.08 (d, J = 2.8 Hz, 1H), 6.21 (dd, J = 9.1, 2.8 Hz, 1H), 7.06 (bs, 2H), 7.52 (d, J = 9.1 Hz, 1H). LCMS (ESI) m/z 234 $(M + H)^+$.

2. Registry Numbers (RN). Methylhydrazine (RN, 60−34−4), hydrazine monohydrate (RN, 7803−57−8), phenylhydrazine (RN, 100−63−0), 2,2,2-trifluoroethylhydrazine soln 70% in water (RN, 5042−30−8), *N*,*N*-dimethylformamide diisopropyl acetal (RN, 18503−89−4), phenylguanidine carbonate salt (RN, 14018−90−7), cyclohexanol (RN, 108−93−0), 4-hydroxy-1-methylpiperidine (RN, 106−52−5), 1-(2-hydroxyethyl)-piperidine (RN, 3040−44−6), triphenylphosphine polymer bound (RN, 39319−11−4), methylamine (RN, 74−89−5), cyclopentylamine (RN, 1003−03−8), phenylamine (RN, 62−53−3), guanidine carbonate salt (RN, 593−85−1), 2-aminobenzotrifluoride (RN, 88−17−5), 3-aminobenzotrifluoride (RN, 89−16−8), 4-aminobenzotrifluoride (RN, 455−14−1), 2-aminoacetophenone (RN, 551−93−9), 3-aminoacetophenone (RN, 99−03−6), 4-aminoacetophenone (RN, 99−92−3), *o*-anisidine (RN, 90−04−0), *m*-anisidine (RN, 536−90−3), *p*-anisidine (RN, 104−94−9), *o*-nitroaniline (RN, 88−74−4), *m*-nitroaniline (RN, 99−09−2), *p*-nitroaniline (RN, 100−01−6), *o*-toluidine (RN, 95−53−4), 2-(methylthio)aniline (RN, 2987−53−3), *N*-methyl-1,2-phenylenediamine (RN, 4760−44−3), 2-fluoroaniline (RN, 348−54−9), 2-isopropylaniline (RN, 643−28−7), methylantranilate (RN, 134−20−3), 2-aminobenzamide (RN, 88−68−6), 2-aminobenzenesulfonamide (RN, 3306−62−5), 2-aminobiphenyl (RN, 90−41−5), 2-aminodiphenyl ether (RN, 2688−84−8), 2-benzylaniline (RN, 28059−64−5), *N*-phenyl-2-phenylenediamine (RN, 534−85−0), 2-aminodiphenylsulfide (RN, 1134−94−7), 2-aminobenzophenone (RN, 2835−77−0), 4-bromo-2-methoxyaniline (RN, 59557−91−4), 5-bromo-2-methoxyaniline (RN, 6358−77−6), 4′-fluoro-2′-hydroxyacetophenone (RN, 1481−27−2), 1-(2-amino-5-bromophenyl)ethanone (RN, 29124−56−9), 1-(2-amino-6-chlorophenyl)ethanone (RN, 20895−91−4).

3. Protein Production and Characterization. $Plk1_{36-345}$ has been expressed in H5 insect cells as GST tag protein. The tag has been removed by enzymatic digestion with PreScission Protease (GE), and the protein has been purified by ion exchange column. Plk1 has then been submitted to limited lysine methylation using a reductive methylation kit (Jena Biosciences). After methylation, the protein has been gel filtered to remove excess of reagents. Level of methylation has been assessed by LC/MS analysis on a 1100 Agilent instrument using a Vydac C-4 column (2.1 mm × 250 mm, 5 μm, poresize 300 Å) Positive ion ESI mass spectra were obtained using 1946 single quadrupole mass spectrometer (Agilent) with an orthogonal ESI.

4. Crystallography Methods. In the final optimized crystallization conditions, methylated-$Plk1_{36-345}$ at a concentration of 20 mg/mL was incubated with 10 mM AMP-PNP and 10 mM

$MgCl_2$ prior to crystallization via the vapor diffusion method. Crystallization was done by mixing 0.5 μL of protein mixture with 0.5 μL of a reservoir solution consisting of 1.2 M Na/K tartrate and 0.1 M MES buffer at pH 6.0. After one week at 4 °C, Zn acetate was added to the drops at a final concentration of about 25 mM, and the drops were immediately seeded using crystals of the methylated-$Plk1_{36-345}$:AMP-PNP complex. Crystals grew in a few days. One crystal was soaked for three hours in a solution containing 1.2 M Na/K tartrate, 0.1 M MES pH 6.0, 20% glycerol, and 1 mM compound **49** and flash-cooled in liquid nitrogen. Diffraction data were collected at beamline ID14-EH3 at the European Synchrotron Radiation Facility (Grenoble, France). Data were processed with MOSFLM[41] and programs of the CCP4 suite.[42] The structure has been solved by molecular replacement using MOLREP[43] and an in-house available structure of $PLK1_{36-345}$ in complex with AMP-PNP as a search model. Crystals belong to space group $P3_221$ and contain one molecule in the asymmetric unit. The structure was refined with Refmac5,[44] water molecules were added with Arp,[45] and model building was done with Coot.[46] The final model has $R_{factor} = 0.210$ and $R_{free} = 0.298$. All structural figures were generated with PyMol (http://pymol.sourceforge.net/).

5. Kinase Assays. The inhibitory activity of putative kinase inhibitors and the potency of selected compounds were determined using a transphosphorylation assay. Specific peptide or protein substrates were transphosphorylated by their specific serine-threonine or tyrosine kinase, in the presence of ATP traced with ^{33}P-γ-ATP, at optimized buffer and cofactors conditions. At the end of the phosphorylation reaction, more than 98% unlabeled ATP and radioactive ATP was captured by adding an excess of the ion exchange dowex resin; the resin then settles down to the bottom of the reaction plate by gravity. Supernatant, containing the phosphorylated substrate, was subsequently withdrawn and transferred into a counting plate, followed by evaluation by β-counting. Inhibitory potency evaluation for all the tested kinases was performed at 25 °C using a 60 min end-point assay where the concentrations of ATP and substrates were kept equal to $2 \times \alpha K_m$ and saturated ($> 5 \times \alpha K_m$), respectively.[47]

Plk1 Assay. Inhibition of Plk1 kinase activity was assessed using a Dowex resin capture technique. In this assay, 85 μM αCasein (Sigma) was phosphorylated by 3 nM Plk1 (2−345) in the presence of ATP (40 μM) traced with ^{33}P-γ-ATP in kinase buffer (50 mM Hepes pH = 7.9, 10 mM beta glycerylphosphate, 1 mM DTT, 3 μM $NaVO_3$, 10 mM $MgCl_2$, 0.2 mg/mL BSA) for 60 min. By addition of an acidic suspension of Dowex resin (SIGMA, custom-prepared resin Dowex 1 × 8200−400 mesh equilibrated in 150 mM sodium formate, pH = 3.0) the unreacted ATP was captured and separated from the supernatant which contained the phosphorylated substrate: this was then transferred into a new plate for radioactivity counting. The assay is run in a robotized format on 384-well plates.

Plk2 Assay. Inhibition of Plk2 kinase activity was assessed using a Dowex resin capture technique. In this assay, 175 μM αCasein (Sigma) was phosphorylated by 5 nM Plk2 (2−375) in the presence of ATP (200 μM) traced with ^{33}P-γ-ATP in kinase buffer (50 mM Hepes pH = 7.9, 10 mM beta glycerylphosphate, 1 mM DTT, 3 μM $NaVO_3$, 5 mM $MgCl_2$, 0.2 mg/mL BSA) for 60 min. By addition of an acidic suspension of Dowex resins (SIGMA, custom-prepared resin Dowex 1 × 8200−400 mesh equilibrated in 150 mM sodium formate, pH = 3.0) the unreacted ATP is captured and separated from the supernatant which contained the phosphorylated substrate: this was then transferred into a new plate for radioactivity counting. The assay is run in a robotized format on 384-well plates.

Plk3 Assays. Inhibition of Plk3 kinase activity was assessed using a Dowex resin capture technique. In this assay, 110 μM αCasein (Sigma) was phosphorylated by 0.5 nM Plk3 (2−355) in the presence of ATP (50 μM) traced with ^{33}P-γ-ATP in kinase buffer (50 mM Hepes pH = 7.9, 10 mM beta glycerylphosphate, 1 mM DTT, 3 μM $NaVO_3$, 5 mM $MgCl_2$, 0.2 mg/mL BSA) for 60 min at room temperature. By addition of an acidic suspension of Dowex resin (SIGMA, custom-prepared resin Dowex 1 × 8 200−400 mesh equilibrated in 150 mM sodium formate, pH = 3.0), the unreacted ATP was captured and separated from the supernatant which contained the phosphorylated substrate: this was then transferred onto a new plate for radioactivity counting. The assay is run in a robotized format on 384-well plates.

6. Cell Cycle Analysis. Floating cells in the medium (usually mitotic or in apoptosis) or released during PBS washes were collected, added to adherent cells, detached from the plastic by mild treatment with trypsin, and fixed in 70% ethanol/PBS. Cells were washed with PBS to remove fixative and stained with 25 μg/mL propidium iodide, 5 μg/mL RNase, and 0.125 μg/mL Nonidet P40. Cells were kept at room temperature for 60 min in the dark and were analyzed using a flow cytometry BD FACSCalibur system (BD Biosciences). DNA content analysis was performed on ≥10000 gated cells and DNA histograms were analyzed using ModFit LT (Verity Software House, Topsham, ME).

7. Western Blot Analysis. Cells were lysed in 125 mmol/L Tris-HCl (pH = 6.8) and 2% SDS and heated for 10 min at 95 °C. Total proteins (20 μg), as determined by BCA protein assay (Pierce, Rockford, IL), were separated by 4−12% SDS-PAGE. Immunoblot analysis was done using the following antibodies: anti-TCTP (BD Transduction Laboratories, Franklin Lakes, NJ), antiphosphorylated TCTP Ser46 (custom-made by Zymed, San Francisco, CA), antiphosphorylated histone H3 Ser10 (Upstate Biotechnology, Lake Placid, NY), anti-histone H3 (Abcam, Cambridge, United Kingdom), antiphosphorylated NPM Thr199 (Cell Signaling, Danvers, MA), anti-caspase-3 (Cell Signaling Technology, Inc.) and anti-GAPDH (FL-335) (Santa Cruz Biotechnology, Inc.). Immunoblot was carried out according to standard methods. Amersham ECL (GE Healthcare) was used for detection.

8. Immunohistochemisty and siRNA. Immunohistochemisty and siRNA experiments were performed as previously described.[48,49]

9. Cell Culture. A2780 human ovarian cancer cells and their resistant variants, A431 epidermoid carcinoma, OPM-2 and NCI-H929 myeloma, KARPAS-299 and Jurkat lymphoma cells, KU812 leukemia, and HEL erythroleukemia lines were cultured in RPMI1640 supplemented with 10% fetal bovine serum, HCT116 colon adenocarcinoma in McCoy's, LoVo colon adenocarcinoma, and its doxorubicin resistant derivative line in HAM's F12, Mia-PaCa-2, and Panc-1 pancreatic adenocarcinoma in DMEM supplemented with 10% fetal bovine serum, MCF7 in EMEM plus 10% fetal bovine serum, and 1% NEAA, NHDF in fibroblast basal medium kit supplemented with the appropriate growth factors (PromoCell), 1 ng/mL bFGF, and 10% fetal bovine serum. A2780, A2780/ADR, A2780/cis, A431, HCT116, LoVo, MCF7, Mia-PaCa-2 lines were obtained from the ECACC, KARPAS-299, and OPM-2 from the DSMZ collection, A2780 1A9, and A2780 1A9/PTX22 were kind gifts from Professor R. Giavazzi (Mario Negri Institute, Milan), NHDF were purchased from PromoCell, the resistant variant LoVo/DX was generated growing its parent cell line in the presence of 100 ng/mL doxorubicin, all other lines were obtained from ATCC collection.

10. Inhibition of Cell Proliferation. Cells were seeded into 384-well white plates at a density of 3000 cells/well for adherent and 5000 cells/well for nonadherent lines in complete growth medium and treated with compounds dissolved in 0.1% DMSO 24 h after the seeding. The cells were incubated at 37 °C and 5% CO_2 and after 72 h of treatment the plates were processed using CellTiter-Glo assay (Promega) following the manufacturer's instruction. CellTiter-Glo is a homogeneous method based on the quantification of the ATP present as an indicator of metabolically active cells. ATP was measured using a system based on luciferase and D-luciferin resulting in light generation. The luminescent signal is proportional to the number of cells present

in culture. Briefly 25 μL/well reagent solution was added and mixed to each well, and after 5 min, the microplates were read in a luminometer. The concentration required to inhibit cell growth by 50% (IC_{50}) was calculated from point-to-point curves using Assay Explorer (MDL) software.

11. High-Throughput Solubility. Nominal 250 μM compounds suspensions/solutions in aqueous ammonium acetate buffer at pH = 7 were prepared on a Multiscreen-GV, 0.2 μm filter plate (Millipore, Billerica, MA). These solutions were stored for 24 h at room temperature to presaturate the membrane filter and to reach a "pseudothermodynamic solubility". Then a premixed solution of acetonitrile/water (40/60 v/v) was stirred, filtered, and diluted (25-fold). The so obtained nominal 10 μM solutions were then analyzed simultaneously by LC-MS/MS with standard solutions for quantification.

12. Metabolic Stability in Human Liver Microsomes (HLM). HLM (BD Gentest, Woburn, MA) at a concentration of 0.8 mg/mL, were preincubated with 1 mM test compound for 5 min at 37 °C in 0.1 M phosphate buffer, pH = 7.4, and then the reactions were initiated by adding warmed NADPH (1 mM). After 0, 5, 10, and 30 min incubations, the reactions were stopped with a double volume of ice-cold acetonitrile. The samples were centrifuged for 20 min at 1500 rpm, and the amount of compound remaining was determined with LC-MS/MS. The in vitro Cl_{int} was calculated and then scaling factors have been used to estimate the in vivo Cl_{int} according to the following equation:

$$Cl_{intinvivo} = (0.693/t_{1/2})(\text{incubationvolume/mgHLM})$$
$$(\text{mgHLM/(gliver)/kgbodyweight})$$

where mg HLM/g of liver = 45 mg and g liver/kg body weight (human) = 20 g.

13. Intrinsic Clearance Determination in Rat Hepatocytes (RH). Cl_{int} determinations in rat hepatocytes (prepared in-house) suspensions were performed in Leibovitz's medium, with 1.0×10^6 viable cells/mL and 1 mM test compound, at 37 °C. The reactions were stopped at 0, 10, 30, 60, and 90 min with a double volume of ice-cold acetonitrile. The samples were centrifuged at 700*g* for 20 min and then the amount of compound remaining was determined with LC-MS/MS. The in vitro Cl_{int} was calculated, and then scaling factors were used to estimate the in vivo Cl_{int} according to the following equation:

$$Cl_{intinvivo} = (0.693/t_{1/2})(\text{incubationvolumeofRH})$$
$$(\text{numberofRH/gliver})/(\text{gliver/kgbodyweight})$$

where number of RH/g of liver = 1×10^8 and g liver/kg body weight (rat) = 44 g.

14. Cell Permeability. Parallel Artificial Membrane Permeability Assay (PAMPA). A 96-well filtration plate, MAIP N45 (Millipore, Billerica, MA), was used as support for 4 μL of the membrane forming solution and as acceptor plate, filled with 200 μL of blank buffer solution, HBSS pH = 7.4 with HEPES (Gibco BRL). The membrane forming solution consisted of 15% soy lecithin in *n*-dodecane. Then 200 μL of donor solution, containing the compound at 10 μM, in HBSS pH 7.4 with HEPES, were placed in a 96-well donor plate (p-ION, Woburn, MA) and then the acceptor plate was placed on top of the donor plate. The obtained "sandwich" was incubated at 37 °C for 4 h. After incubation, acceptor, donor, and initial donor solution (reference) were analyzed by LC-MS/MS. Compound apparent Permeability (P_{app}) is calculated using the following formula:

$$P_{app}(\text{cm/s}) = \{-\ln[1 - C_r(t)/C_{eq}]\}/[A(1/V_d + 1/V_r)t]$$

where A is the filter area, V_d is the donor volume, V_r is the receiver volume, t is the incubation time (s), $C_r(t)$ is the concentration in the receiver at time t, $C_d(t)$ is the concentration in the donor at time t, and C_{eq} is the equilibrium concentration $[C_d(t)\,(V_d + C_r(t))V_r]/(V_d + V_r)$.

Human Colon Adenocarcinoma Cells (Caco-2). Caco-2 cells (American Type Culture Collection, Rockville, MD) monolayers on 24-transwell plates were preincubated at 37 °C and pH = 7.4 with HBSS containing 25 mM Hepes (Gibco BRL). Permeability studies were performed in two transport directions, apical to basolateral (absorption) and basolateral to apical (secretion), adding fresh donor solution containing 10 μM of test compound in HBSS on the donor side while placing compound-free HBSS on the receiver side. The 24-transwell plates were placed on a heated plate shaker. After 120 min, the solutions from the receivers and donors chambers were collected and aliquots were analyzed by LC-MS/MS. The Permeability coefficients (P_{app}) were calculated using the following the equation:

$$P_{app}(\text{cm/s}) = (dCV_r)/(dt\,AC_o)$$

where: C_o is the initial concentration, dC/dt is the flux across the monolayer, V_r is the volume of the receiver compartment, and A is the membrane surface area.

15. In Vivo pharmacokinetics Nude Mouse. The pharmacokinetic profile of the compounds was investigated in overnight fasted male nude mice following a single dose given intravenously (iv) or orally (po). The compound was formulated as in situ hydrochloride salt in glucosate solution as vehicle. A total of six mice were treated (three for each leg). Blood samples of each mouse were collected from the saphenous vein at predose, 0.083, 0.5, 1, 6, and 24 h postdosing following iv dosing, and at predose, 0.25, 0.5, 1, 6, and 24 h following oral dosing. Samples were centrifuged at 10000 rpm for 3 min at 4 °C, and the plasma was stored at −80 °C until analysis. Samples were analyzed by LC/MS/MS technique.

Pharmacokinetic Noncompartmental Data Analysis. The pharmacokinetic parameters were derived by noncompartmental methods using the WinNonlin software program. The highest concentration C_{max} and the time to peak t_{max} were read as the coordinates of the highest observed concentration. The terminal half-life ($t_{1/2,z}$) was calculated by the formula $t_{1/2,z} = \ln(2)/\lambda z$, where λz is the slope of the terminal linear phase of natural-log concentrations vs time curve. The choice of the points on the terminal phase was based on visual inspection of the data. The area under the plasma level vs time curve, AUC_∞, was calculated by the linear trapezoidal rule up to the last detectable concentration $C(t_z)$ and beyond that time by extrapolation from $C(t_z)$ assuming monoexponential decay, using the following formula: $AUC = AUC(0 - t_z) + C(t_z)/\lambda_z$. The following formulas were applied for the estimate of plasma clearance (CL) and volume of distribution at steady state (V_{ss}). $CL = dose/AUC_\infty$; $MRT = AUMC/AUC_\infty$; $V_{ss} = CL \cdot MRT$; $AUMC = AUMC(0 - t_z) + C(t_z)\,t_z/\lambda_z + C(t_z)/\lambda_z^2$, with $AUMC(0 - t_z)$ calculated using the linear trapezoidal rule on $C \cdot t$ vs t plots. The oral bioavailability (expressed as percent) was estimated by the ratio of dose-normalized AUC_∞ values after oral and iv dose.

16. LC-MS/MS Analyses. Analyses were performed with an LC-MS/MS system which consisted of an 1100 binary pump (Agilent Technologies, Santa Clara, CA), an HTS-PAL autosampler (CTC Analytics AG, Zwingen, Switzerland), and an API 2000 mass spectrometer (AB/MDS-SCIEX, Concord, ON, Canada). Chromatography was performed on a SB-C8 guard-column, 5 μM, 12.5−4.6 mm (Agilent Technologies, Santa Clara, CA), eluted at a flow rate of 0.6 mL/min. Mobile phase A was 95% ammonium formate 10 mM, pH 4.0 and 5% acetonitrile, while mobile phase B was 5% ammonium formate 10 mM, pH 4.0 + 95% acetonitrile. Compound elution was obtained at a flow rate of 0.6 mL/min with a step gradient from 0 to 100% B at time zero. Detection was done by using a Turbo IonSpray source in the multiple-reaction monitoring MS/MS mode.

17. Evaluation of Antitumor Efficacy. BALB/c nu/nu male mice from Harlan Italy, 6 weeks old weighing 21−30 g, were maintained in cages with paper filter covers, food, sterilized bedding, and acidified water. HCT116 cells (from American

Type Culture Collection) were inoculated subcutaneously. The treatments started when the tumors were measurable; mean tumor weight for all the groups was 0.170 g and compound **49** was suspendend in methocel. Treatments were administered orally once a day at day 13, 14, 17, 18, 22, 23, 27, and 28. In the control group, animals were treated with the vehicle with the same scheduling. The tumor growth was evaluated every three days. Tumour dimension was regularly measured by calipers during the experiments, and the tumor mass was calculated as described.[50]

The tumor growth inhibition (TGI, %) was calculated according to the equation: % TGI = 100 − (mean tumor weight of treated group/mean tumor weight of control group) × 100. Toxicity was evaluated on the basis of the body weight reduction. Mice were sacrificed when the tumors reached a volume that hampered them.

Acknowledgment. The authors are grateful to the group of assay development of Nerviano Medical Sciences and to Fulvia Roletto for the biochemical assay on Plk2 and Plk3. We thank Walter Moretti and Dania Tesei for their skilled synthetic chemistry support, Daniele Pezzetta, Cristina Ciocca for ADME characterization and solubilily data, Marina Fasolini for her support in the crystallographic screening, Stefania Re Depaolini, Simona Rizzi for constructs production, Francesco Sola and Maria Laura Giorgini for immunofluorescence images and for apoptosis evaluation, Francesco Colotta, Daniele Donati, Eduard Felder, Arturo Galvani, Antonella Isacchi, Nicola Mongelli, Mario Varasi for discussion and support.

Note Added after ASAP Publication. This paper was published on April 16, 2010 with a production error in the Results and Discussion section. The revised version was published on April 21, 2010.

Supporting Information Available: X-ray crystallographic studies of compound **49**. This material is available free of charge via the Internet at http://pubs.acs.org.

References

(1) Donaldson, M. M.; Tavares, A. A.; Hagan, I. M.; Nigg, E. A.; Glover, D. M. The mitotic roles of Polo-like kinase. *J. Cell. Sci.* **2001**, *114*, 2357–2358.
(2) Glover, D. M.; Hagan, I. M; Tavares, A. A. Polo-like kinases: a team that plays throughout mitosis. *Genes Dev.* **1998**, *12*, 3777–3787.
(3) Nigg, E. A. Polo-like kinases: positive regulators of cell division from start to finish. *Curr. Opin. Cell Biol.* **1998**, *10*, 776–783.
(4) Kumagai, A.; Dunphy, W. G. Purification and molecular cloning of Plx1, a Cdc25-regulatory kinase from *Xenopus* egg extracts. *Science* **1996**, *273*, 1377–1380.
(5) Barr, F. A.; Sillje, H. H; Nigg, E. A. Polo-like kinases and the orchestration of cell cycle division. *Nat. Rev. Mol. Cell Biol.* **2004**, *5*, 429–440.
(6) van Vugt, M. A.; van de Weerdt, B. C.; Vader, G.; Janssen, H.; Calafat, J.; Klompmaker, R.; Wolthuis, R. M.; Medema, R. H. Polo-like kinase-1 is required for bipolar spindle formation but is dispensable for anaphase promoting complex/Cdc20 activation and initiation of cytokinesis. *J. Biol. Chem.* **2004**, *279*, 36841–36854.
(7) Nakajima, H.; Toyoshima-Morimoto, F.; Taniguchi, E.; Nishida, E. Identification of a consensus motif for Plk (Polo-like kinase) phosphorylation reveals Myt1 as a Plk1 substrate. *J. Biol. Chem.* **2003**, *278*, 25277–25280.
(8) Bartholomew, C. R.; Woo, S. H.; Chung, Y. S.; Jones, C.; Hardy, C. F. Cdc5 interacts with the Wee1 kinase in budding yeast. *Mol. Cell. Biol.* **2001**, *21*, 4949–4959.
(9) Qian, Y. W.; Erikson, E.; Taieb, F. E.; Maller, J. L. The polo-like kinase Plx1 is required for activation of the phosphatase Cdc25C and cyclin B-Cdc2 in *Xenopus* oocytes. *Mol. Biol. Cell* **2001**, *12*, 1791–1799.
(10) Wolf, G.; Elez, R.; Doermer, A.; Holtrich, U.; Ackermann, H.; Stutte, H. J.; Altmannsberger, H. M.; Rübsamen-Waigmann, H.; Strebhardt, K. Prognostic significance of polo-like kinase (PLK) expression in non-small cell lung cancer. *Oncogene* **1997**, *14*, 543–549.
(11) Weichert., W; Kristiansen, G.; Schmidt, M.; Gekeler, V.; Noske, A.; Niesporek, S.; Dietel, M.; Denkert, C. Polo-like kinase 1 expression is a prognostic factor in human colon cancer. *World J. Gastroenterol.* **2005**, *11*, 5644–5650.
(12) Weichert, W.; Schmidt, M.; Gekeler, V.; Denkert, C.; Stephan, C.; Jung, K.; Loening, S.; Dietel, M.; Kristiansen, G. Polo-like kinase 1 is overexpressed in prostate cancer and linked to higher tumor grades. *Prostate* **2004**, *60*, 240–245.
(13) Weichert, W.; Denkert, C.; Schmidt, M.; Gekeler, V.; Wolf, G.; Kobel, M.; Dietel, M.; Hauptmann, S. Polo-like kinase isoform expression is a prognostic factor in ovarian carcinoma. *Br. J. Cancer* **2004**, *90*, 815–821.
(14) Weichert, W.; Kristiansen, G.; Winzer, K. J.; Schmidt, M.; Gekeler, V.; Noske, A.; Muller, B. M.; Niesporek, S.; Dietel, M.; Denkert, C. Polo-like kinase isoforms in breast cancer: expression patterns and prognostic implications. *Virchows Archiv.* **2005**, *446*, 442–450.
(15) Knecht, R.; Elez, R.; Oechler, M.; Solbach, C.; von Ilberg, C.; Strebhardt, K. Prognostic Significance of Polo-like Kinase (PLK) Expression in Squamous Cell Carcinomas of the Head and Neck. *Cancer Res.* **1999**, *59*, 2794–2797.
(16) Schmit, T. L.; Zhong, W.; Setaluri, V.; Spiegelman, V. S.; Ahmad, N. Targeted Depletion of Polo-Like Kinase (Plk) 1 Through Lentiviral shRNA or a Small-Molecule Inhibitor Causes Mitotic Catastrophe and Induction of Apoptosis in Human Melanoma Cells. *J. Invest. Dermatol.* **2009**, *129*, 2843–2853.
(17) Lane, H. A.; Nigg, E. A. Antibody microinjection reveals an essential role for human polo-like kinase 1 (Plk1) in the functional maturation of mitotic centrosomes. *J. Cell. Biol.* **1996**, *135*, 1701–1713.
(18) Matthess, Y.; Kappel, S.; Spaenkuch, B.; Zimmer, B.; Kaufmann, M.; Strebhardt, K. Conditional inhibition of cancer cell proliferation by tetracycline-responsive, H1 promoter-driven silencing of PLK1. *Oncogene* **2005**, *24*, 2973–2980.
(19) Nogawa, M.; Yuasa, T.; Kimura, S.; Tanaka, M.; Kuroda, J.; Sato, K.; Yokota, A.; Segawa, H.; Toda, Y.; Kageyama, S.; Yoshiki, T.; Okada, Y.; Maekawa, T. Intravesical administration of small interfering RNA targeting PLK-1 successfully prevents the growth of bladder cancer. *J. Clin. Invest.* **2005**, *115*, 978–985.
(20) Spankuch-Schmitt, B.; Wolf, G.; Solbach, C.; Loibl, S.; Knecht, R.; Stegmuller, M.; von Minckwitz, G.; Kaufmann, M.; Strebhardt, K. Downregulation of human polo-like kinase activity by antisense oligonucleotides induces growth inhibition in cancer cells. *Oncogene* **2002**, *21*, 3162–3171.
(21) Spankuch-Schmitt, B.; Bereiter-Hahn, J.; Kaufmann, M.; Strebhardt, K. Effect of RNA silencing of polo-like kinase-1 (PLK1) on apoptosis and spindle formation in human cancer cells. *J. Natl. Cancer Inst.* **2002**, *94*, 1863–1877.
(22) Liu, X.; Lei, M.; Erikson, R. L. Normal cells, but not cancer cells, survive severe Plk1 depletion. *Mol. Cell. Biol.* **2006**, *26*, 2093–2108.
(23) Kauselmann, G.; Weiler, M.; Wulff, P.; Jessberger, S.; Konietzko, U.; Scafidi, J.; Staubli, U.; Bereiter-Hahn, J.; Strebhardt, K.; Kuhl, D. The polo-like protein kinases Fnk and Snk associate with a $Ca^{(2+)}$ and integrin-binding protein and are regulated dynamically with synaptic plasticity. *EMBO J.* **1999**, *18*, 5528–5539.
(24) Gumireddy, K.; Reddy, M. W.; Cosenza, S. C.; et al. ON01910, a non-ATP-competitive small molecole inhibitor of Plk1, is a potent anticancer agent. *Cancer Cell* **2005**, *7*, 275–286.
(25) Mross, K.; Frost, A.; Steinbild, S.; Hedbom, S.; Rentschler, J.; Kaiser, R.; Rouyrre, N.; Trommeshauser, D.; Hoesl, C. E.; Munzert, G.; Phase, I dose escalation and pharmacokinetic study of BI 2536, a novel Polo-like kinase 1 inhibitor, in patients with advanced solid tumors. *J. Clin. Oncol.* **2008**, *26*, 5511–5517.
(26) Rudolph, D.; Steegmaier, M.; Hoffmann, M.; Grauert, M.; Baum, A.; Quant, J.; Haslinger, C.; Garin-Chesa, P.; Adolf, G. A. BI6727, A Polo-like kinase inhibitor with improved pharmacokinetic profile and broad antitumor activity. *Clin. Cancer Res.* **2009**, *15*, 3094–3102.
(27) Sutton, D.; Diamond, M.; Faucette, L.; Giardiniere, M.; Zhang, S.; Gilmartin, A.; Salovich, J.; Cheung, M.; Kuntz, K.; Laquerre, S.; Pearl Huang, P.; Jackson, J. R. Efficacy of GSK461364, a selective Plk1 inhibitor, in human tumor xenograft models. AACR Annual Meeting, Los Angeles, Apr 14−18, 2007, Vol. *48*, poster 5388.
(28) Blagden, S.; Olmons, D.; Sharma, R.; Barriuso, J.; Medani, H.; Versola, M.; Murray, S.; Smith, D. A. Dar, M. M. de Bono, J. S. A phase I first-in-human study of the polo-like kinase 1 selective inhibitor, GSK-461364, in patients with advanced solid tumors. Book of Abstracts, EORTC-NCI-AACR, Geneva, Oct 21−24, 2008, poster 431.

(29) Schoffsky, P. Polo-Like Kinase (PLK) Inhibitors in Preclinical and Early Clinical Development in Oncology. *Oncologist* **2009**, *14*, 559–570.
(30) Caruso, M.; Beria, I.; Brasca, M. G.; Ferguson, R.; Posteri, H.; Valsasina, B. Substituted pyrazolo-quinazoline derivatives, process for their preparation and their use as kinase inhibitors. Patent WO 2008/074788, 2008.
(31) Brasca, M. G.; Amboldi, N.; Ballinari, D.; Cameron, A.; Casale, E.; Cervi, G.; Colombo, M.; Colotta, F.; Croci, V.; D'Alessio, R.; Fiorentini, F.; Isacchi, A.; Mercurio, C.; Moretti, W.; Panzeri, A.; Pastori, W.; Pevarello, P.; Quartieri, F.; Roletto, F.; Traquandi, G.; Vianello, P.; Vulpetti, A.; Ciomei, M. Identification of *N*,1,4,4-Tetramethyl-8-{[4-(4-methylpiperazin-1-yl)phenyl]amino}-4,5-dihydro-1*H*-pyrazolo[4,3-*h*]quinazoline-3-carboxamide (PHA-848125), a Potent, Orally Available Cyclin Dependent Kinase Inhibitor. *J. Med. Chem.* **2009**, *52*, 5152–5163.
(32) Mizuno, M.; Yamano, M. New practical one-pot conversion of phenols to anilines. *Org. Lett.* **2005**, *7*, 3629.
(33) Kothe, M.; Kohls, D.; Low, S.; Coli, R.; Cheng, A. C.; Jacques, S. L.; Johnson, T. L.; Lewis, C.; Loh, C.; Nonomiya, J.; Sheils, A. L.; Verdries, K. A.; Wynn, T. A.; Kuhn, C.; Ding, Y. Structure of the catalytic domain of human Polo-like kinase. *Biochemistry* **2007**, *46*, 5960–5971.
(34) Coordinates of the Plk1 complexes with compounds **49** have been deposited in the Protein Data Base under accession code 3KB7, together with the corresponding structure factor files.
(35) Knight, J. D. R.; Hamelberg, D.; McCammon, J. A.; Kothary, R.. The role of conserved water molecules in the catalytic domain of protein kinases. *Proteins: Struct., Funct., and Bioinform.* **2009**, *76*, 527–535.
(36) Kornev, A. P.; Taylor, S. S.; Ten Eyck, L. F. A helix scaffold for the assembly of active protein kinases. *Proc. Natl. Acad. Sci. U.S.A.* **2008**, *105*, 14377–14382.
(37) Kothe, M.; Kohls, D.; Low, S.; Coli, R.; Rennie, G. R.; Feru, F.; Kuhn, C.; Ding, Y. Selectivity-determining residues in Plk1. *Chem. Biol. Drug Des.* **2007**, *70*, 540–546.
(38) Emmitte, K. A.; Adjebang, G. M.; Andrews, C. W.; Badiang Alberti, J. G.; Bambal, R.; Chamberlain, S. D.; Davis-Ward, R. G.; Dickson, H. D.; Hassler, D. F.; Hornberger, K. R.; Jackson, J. R.; Kuntz, K. W.; Lansing, T. J.; Mook, R. A., Jr.; Nailor, K. E.; Pobanz, M. A.; Smith, S. C.; Sung, C.; Cheung, M. Design of potent thiophene inhibitors of polo-like kinase 1 with improved solubility and reduced protein binding. *Bioorg. Med. Chem. Lett.* **2009**, *19*, 1694–1697.
(39) Yarm, F. R. Plk phosphorylation regulates the microtubule-stabilizing protein TCTP. *Mol. Cell. Biol.* **2002**, *22*, 6209–6221.
(40) Colombo, M.; Riccardi-Sirtori, F.; Rizzo, V. A fully automated method for accurate mass determination using high-performance liquid chromatography with a quadrupole/orthogonal acceleration time-of-flight mass spectrometer. *Rapid Commun. Mass Spectrom.* **2004**, *18*, 511–517.
(41) Leslie, A. G. W. Integration of macromolecular diffraction data. *Acta Crystallogr., Sect. D: Biol. Crystallogr.* **1999**, *55*, 1696–1702.
(42) Bailey, S. The CCP4 suite: programs for protein crystallography. *Acta Crystallogr., Sect. D: Biol. Crystallogr.* **1994**, *50*, 760–763.
(43) Vagin, A.; Teplyakov, A.. MOLREP: an automated program for molecular replacement. *J. Appl. Crystallogr.* **1997**, *30*, 1022–1025.
(44) Murshudov, G. N.; Vagin, A. A.; Dodson, E. J. Refinement of macromolecular structures by the maximum-likelihood method. *Acta Crystallogr., Sect. D: Biol. Crystallogr.* **1997**, *53*, 240–255.
(45) Lamzin, V. S.; Wilson, K. S. Automated refinement of protein models. *Acta Crystallogr., Sect. D: Biol. Crystallogr.* **1993**, *49*, 129–47.
(46) Emsley, P.; Cowtan, K. Coot: model-building tools for molecular graphics. *Acta Crystallogr., Sect. D: Biol. Crystallogr.* **2004**, *60* (12, Pt. 1), 2126–2132.
(47) Pevarello, P.; Brasca, M. G.; Amici, R.; Orsini, P.; Traquandi, G.; Corti, L.; Piutti, C.; Sansonna, P.; Villa, M.; Pierce, B. S.; Pulici, M.; Giordano, P.; Martina, K.; Fritzen, E. L.; Nugent, R. A.; Casale, E.; Cameron, A.; Ciomei, M.; Roletto, F.; Isacchi, A.; Fogliatto, G. P.; Pesenti, E.; Pastori, W.; Marsiglio, A.; Leach, K. L.; Clare, P. M.; Fiorentini, F.; Varasi, M.; Vulpetti, A.; Warpehoski, M. A. 3-Aminopyrazole inhibitors of CDK2/cyclin A as antitumor agents. 1. Lead finding. *J. Med. Chem.* **2004**, *47*, 3367–3380.
(48) Carpinelli, P.; Ceruti, R.; Giorgini, M. L.; Cappella, P.; Gianellini, L.; Croci, V.; Degrassi, A.; Texido, G.; Rocchetti, M.; Vianello, P.; Rusconi, L.; Storici, P.; Zugnoni, P.; Arrigoni, C.; Soncini, C.; Alli, C.; Patton, V.; Marsiglio, A.; Ballinari, D.; Pesenti, E.; Fancelli, D.; Moll, J. PHA-739358, a potent inhibitor of Aurora kinases with a selective target inhibition profile relevant to cancer. *Mol. Cancer Ther.* **2007**, *6*, 3158–3168.
(49) Siomi, H.; Siomi, M. On the road to reading the RNA-interference code. *Nature* **2009**, *457*, 396–404.
(50) Bjornsson, T. D.; Callaghan, J. T.; Einolf, H. J.; Fischer, V.; Gan, L.; Grimm, S.; Kao, J.; King, S. P.; Miwa, G.; Ni, L.; Kumar, G.; McLeod, J.; Obach, S. R.; Roberts, S.; Roe, A.; Shah, A.; Snikeris, F.; Sullivan, J. T.; Tweedie, D.; Vega, J. M.; Walsh, J.; Wrighton, S. A. The conduct of in vitro and in vivo drug-drug interaction studies: A PhRMA perspective. *J. Clin. Pharm.* **2003**, *43*, 443–469.